FADD and its Phosphorylation Mediate Mitogenic Signaling in Mutant *Kras* Tumors

by

Brittany Bowman

A dissertation submitted in partial fulfillment
of the requirements for the degree of
Doctor of Philosophy
(Biological Chemistry)
in the University of Michigan
2015

Doctoral Committee:

Professor Brian D. Ross, Chair
Professor Alnawaz Rehemtulla
Professor Philip C. Andrews
Professor David G. Beer
Associate Professor Roland Kwok
Assistant Professor Marina Pasca di Magliano

DEDICATION

This is dedicated to my family who encouraged me to pursue science as a career.

AKNOWLEDGEMENTS

I am sincerely grateful to thank Brian Ross and Alnawaz Rehemtulla for not only taking me on as a technician right out of undergrad but also for graduate school. Working for them has allowed me to experience working on many types of basic and translational research. My committee, David Beer, Marina Pasca di Magliano, Roland Kwok, and Phil Andrews were the best thesis committee a graduate student could have. Their suggestions and support were highly valuable over the years. I would like to especially thank Marina for letting me attend her weekly lab meetings where I could expand my background and practice public speaking.

I also have deep gratitude for both Craig and Stefanie Galbán. Without Craig I would not have been given a chance to get into graduate school. He was also a great source to go to for help on imaging. I am greatly appreciative for having gotten to work with Stefanie. She was a great role model, mentor and friend. She was much of the motivation behind this work and without her it would not have been nearly as fun to work on.

Both members of Brian Ross and Al Rehemtulla labs have been great to work with and much of the work presented in this thesis would not have been possible without many of them. I would like to thank Ben Hoff, Kevin Heist, Jen Boes and Carlos Espinoza who greatly helped me with all aspects of imaging. I would also like to thank Katie Sebolt and Mahaveer Swaroop Bhojani for their previous work on this project laying the ground work for this thesis. Also, I would like to thank Hanxiao Wang for being a great friend and colleague. Additionally, thank you to all of the undergraduates who have assisted the lab over the years.

One of the best decisions I have made was in joining the Biological Chemistry department at the University of Michigan. I have enjoyed great conversations with students and professors alike. I would also like to thank the administration staff,

especially Beth Goodwin, as they have been integral in making graduate school as smooth as possible as well.

I am indebted to my husband for everything. Chase was an integral part in supporting me not only through writing, but throughout all of graduate school. He made this process enjoyable with in depth conversations and most importantly was the perfect proofreader. Lastly, I would like to thank my family for also being very supportive of my endeavors.

TABLE OF CONTENTS

LIST OF FIGURES

LIST OF TABLES

ABBREVIATIONS

ADC	→ Adenocarcinoma
Ad-Cre	→ Adenovirus expressing Cre-Recombinase
ALK	→ Anaplastic Lymphoma Kinase
AKT	→ Protein Kinase B
ATI	→ Alveolar type I cell
ATII	→ Alveolar type II cell
AURKA	→ Aurora Kinase A
AURKB	→ Aurora Kinase B
BLI	→ Bioluminescence
BUB1	→ Budding Uninhibited by Benzimidazoles 1
CK1α	→ Casen Kinase 1 alpha
CT	→ Computed Tomography
DD	→ Death Domain
DED	→ Death Effector Domain
EGF	→ Epidermal Growth Factor
EGFR	→ Epidermal Growth Factor Receptor
ERK	→ Extracellular-signal-Regulated Kinase
FADD	→ Fas-Associated Death Domain
FTase	→ Farnsyltransferase
GAP	→ GTPase Activating Proteins
GEF	→ Guanine Exchange Factor
GFP	→ Green fluorescent protein
GSK3β	→ Glycogen Synthase Kinase 3 Beta
H&E (HE)	→ Hematoxylin and Eosin Y
MAPK	→ RAS-mitogen-activated protein kinase
MEF	→ Mouse Embryonic Fibroblast
MDM2	→ Mouse Double Minute 2 homolog
MDM4/X	→ Mouse Double Minute 4/X homolog
MEK	→ Mitogen-activated protein kinase kinase
NES	→ Nuclear Export Sequence
NLS	→ Nuclear Localization Sequence
NSAF	→ Normalized Spectral Abundance Factor
NSCLC	→ Non-Small Cell Lung Cancer
P53	→ Tumor protein p53
PCR	→ Poly-chain reaction
PET	→ Positron Emission Tomography
PI3K	→ Phosphoinositide 3 Kinase

PLK1   → Polo-like Kinase 1
RAL   → Ras-related protein
RIPK1   → Receptor-interacting serine/threonine-protein kinase 1
RIPK3   → Receptor-interacting serine/threonine-protein kinase 3
SOS   → Son of Sevenless
SCC   → Squamous cell carcinoma
SCLC   → Small cell lung cancer
µCT   → Micro-Computed Tomography

CHAPTER 1

INTRODUCTION

1.1 Overview

Lung cancer is the number one cause of cancer related deaths in both men and women in the United States. The current standard of care is unsuccessful in treating these patients, thus new anticancer agents are needed. This section of the thesis will give an overview of the lung and lung cancer as well as therapies currently used and those in clinical trials. Additionally, the signaling pathways whose dysregulation is associated with non-small cell lung cancer, a specific subtype of lung cancer, and a novel target in these pathways, Fas-Associated Death Domain, will be discussed in detail.

1.2 Lung

1.2.1 Structure

The lung is an integral respiratory organ which facilitates the exchange of oxygen and carbon dioxide. The lung consists of five sponge-like lobes, three lobes on the right and two smaller left lobes, which accommodate the heart. Air enters the larynx which passes through the trachea into a system of cartilage lined airways, the bronchi. Air passes through the two main bronchi and then into smaller bronchioles where it reaches sac-like structures called the alveoli the site of gas exchange (**Fig. 1.1**).

The bronchi are composed of cartilage, smooth muscle, and club cells (formerly known as Clara cells). The main function of the bronchi beyond facilitating air to flow into the alveolar sac is to protect the lung from dust and pathogens. This protection is accomplished through the production of a sticky mucus called mucin. To remove the mucin with captured foreign molecules, ciliated club cells move the mucin up and out of

the bronchi and trachea. During infections there is an overproduction of mucin and coughing becomes necessary to remove it **[1, 2]**.

Surrounding the alveoli are thin endothelial cells, fibroblast cells, and a basement membrane (**Fig. 1.2**). Thirty to forty percent of the lung is comprised of fibroblasts **[3].** These cells secrete extracellular matrix components to make up the base membrane adding physical support to the alveoli. Also in the alveolar sac, macrophages function in helping remove dust and pathogens which bypassed the bronchiolar mucin. The alveoli consist of four types of cells, alveolar type I (ATI), alveolar type II (ATII), macrophages, and interstitial fibroblasts. ATI cells are very thin epithelial cells which cover 95% of the alveolus, but only make up 8% of the total cells in the lung **[3]**. ATI are responsible for carrying out gas exchange. ATII cells are cuboidal epithelial cells which are known to produce surfactant. Since the alveoli do not have cartilage or muscle tissue, surfactant is necessary to maintain surface tension keeping the alveolar sac from collapsing **[4]**. ATII cells cover only 5% of the alveolus, but make up 15% of the cells in the lung **[3]**. These cells have been shown to have metabolic functions, but exhibit a slow mitotic rate, which upon injury or growth factors this rate increases. Upon lung injury, ATII cells differentiate into ATI cells for repair **[1, 2]**.

1.3 Lung Cancer

1.3.1 Incidence

Lung cancer is the leading cause of cancer related death worldwide in both men and women. One in four lung cancer patients will succumb to the disease making it more deadly than prostate, breast, colon and pancreatic cancers combined. Lung cancer is the most common cancer in men and the fourth most common cancer in women globally **[5]**. By incidence rate (age-standardized rate) 33.8 per 100,000 men and 13.5 per 100,000 women have lung cancer. However, the rate of incidence in women of North America is higher (35.8-37 per 100,000). In men, this rate is higher (48.5-56.5 per 100,000) in developed countries such as those found in North America, parts of Europe, and East Asia. Rates in less developed countries are lower than in the more developed countries, but are still high at 25.7-32.2 per 100,000 **[5]**. Due to raised awareness of risk factors such as smoking, the incidence and mortality rates are

decreasing **[5]**. However, since the number of smokers has plateaued, these rates will likely remain unchanged.

Although incidence rate has stabilized, the mortality rate has still remained high at 27%. The 5-year survival rate is 15% for all lung cancers. Lung mortality rates in men have declined since 1991 to approximately 61.9 per 100,000. Rates in women started to decline in 2003 (38.5 per 100,000). Unlike incidence rate, location does not seem to play a role in mortality rate **[5]**.The delays in rates between men and women are likely linked to historical shifts in cigarette use since the 1960s **[5, 6]**.

1.3.2 Etiology and Risk Factors:

The etiology of lung cancer has been well studied. **Table 1.1** lists the many known risk factors associated with lung cancer such as environmental and genetic factors. Smoking, air pollution, asbestos, radon, and age are all risk factors associated with lung cancer **[5, 7]**.

Smoking has been the most studied risk factor for the development of lung cancer. The majority of deaths due to lung cancer (80-90%) are thought to be caused by the smoking of tobacco **[5]**. Chemicals present in tobacco smoke, such as polycyclic aromatic hydrocarbons and N-nitroso compounds have been found to be potent carcinogens. These compounds have been associated with G→T transversions as well as to induce mutations in necessary tumor suppressor like *p53* **[5, 6]**. Non-smokers who live with a smoker, and thus are exposed to second hand smoke, also demonstrated higher levels of these compounds, of which directly correlated with the number of cigarettes smoked **[5, 8]**. Non-smokers tend to have G→A transversions resulting in similar phenotypes to smokers but arising from different mutations of the same oncogene or tumor suppressors **[5, 9]**.

The second leading cause of lung cancer is exposure to the radioactive gas radon. Radon naturally diffuses from soil leading to increased domestic exposure. As it decays, radon emits carcinogenic α-particles. Asbestos and other environmental agents such as silica, chromium, nickel, and arsenic have also been implicated as risk factors. (**[5]**, **Table 1.1**)

3

1.3.3 Prognostic Factors in Lung Cancer

Lung cancer has few symptoms until the disease is at a late stage. Symptoms generally involve a chronic cough, shortness of breath, chest pain and weight loss. Lung cancer can be diagnosed during routine examinations by a chest radiograph (chest x-ray) or from a chest CT (computed tomography) scan [10]. Several factors have been identified in lung cancer patients that may help in identifying patients at a higher risk of recurrence and in planning treatment. Important risk factors include: type of the lung cancer, stage and grade of the disease [11].

1.3.3.1 Types of Lung Cancer

There are two types of lung cancer, non-small cell lung cancer (NSCLC) and small cell lung cancer (SCLC) based on appearance of the cell. Over 85% of patients are diagnosed with NSCLC [12]. Several differences between NSCLC and SCLC include location of disease in the lung, cells affected and response to chemotherapy. NSCLC arise primarily in the distal airways whereas SCLC arise closer to main bronchiole airways and is linked with chronic inflammation and smoking as compared to NSCLC. Although SCLC is associated with smoking, the use of cigarettes which include filters and contain less tar correlate with a predisposition with forming adenocarcinomas (ADC), a subtype of NSCLC [10]. This is likely due to the increase in nitrosamines as well as smaller particles that can penetrate the peripheral lung, where ADC tends to form. NSCLC are glandular in nature and express common biomarkers associated with the distal lung. SCLC appears more columnar in nature suggesting a squamous differentiation. SCLC proliferates and metastasizes at a higher rate than NSCLC, although SCLC is more responsive to chemotherapy [10]. Although SCLC is an important disease to study, this thesis will focus primarily on NSCLC due to its refraction to therapy.

1.3.3.2 Histological Grade of NSCLC

Pathological characteristics of NSCLC include ADC, squamous cell carcinoma (SCC) and large cell carcinomas [12]. In general, location of lesions defines the subtype. SCC forms in the lining of the bronchial tubes and likely arises from club cells. As the name implies, SCC morphology is squamous in nature meaning the cells are columnar. SCC stains positively for cytokeratin 5 and 6 as well as SOX2 and p63,

proteins **[12]**. About 50% of patients with NSCLC are diagnosed with ADC **[12]**. This is the most common type of lung cancer in non-smokers. It is believed that these cancers arise from the ATII cells in the alveolar sacs in the periphery of the lung. ADC tends to have glandular features and stain for keratin 7 and NKX2-1, markers consistent with the distal lung **[12]**.

1.3.3.3 Stages of NSCLC

Ascertaining the stage of cancer is currently the most effective method to diagnosing the patient as well as for determining the most suitable treatment options. NSCLC is staged in two ways. The first is clinical staging: the patient undergoes physical examination, biopsies are taken and the patient receives some form of chest imaging such as a CT or PET (positron emission tomography) scan. The second is histological examination of the tumor which provides additional information to the clinical staging. To uniformly stage each patient, the American Joint Committee on Cancer developed TNM staging as shown in **Table 1.2 [13]**. Staging is determined based on tumor size (T), if cancer is present in the lymph nodes (N), and if the cancer has metastasized (M). Numbering 0-4 determines severity. For example: T1 would refer to a patient with one tumor that is larger than 2cm but smaller than 3cm, N2 indicates there is metastasis to the lymph nodes and M0 specifies there are no distant metastasis. After TNM is assessed the patient is diagnosed with a stage 0-IV. Stage 0 refers to cancer in situ while Stage IV refers to cancer that has metastasized to other tissue, e.g. the liver or kidneys. Based on the example given, a patient with T1, N2, and MO would have stage IIIa lung cancer (**Table 1.2**). 40% of new patients are diagnosed with stage IV disease **[11]**. The five-year relative survival rates for patients presenting with stage IA, IB, IIA, IIB, IIIA, IIIB, and IV disease are 49, 45, 30, 31, 14, 5, and 1 percent, respectively **[11]**.

TNM stage is one of the most useful prognostic factors for survival of patients with unresected and resected tumors **[13]**. Other prognostic markers for patients with unresected tumors include age greater than 70, gender, and overall mobility **[11]**. Prognostic factors in patients with resected tumors include nodal stage and histology type. Certain genetic mutations have also been shown to convey prognostic factors as well as resistance to certain drug treatments.

1.3.3.4 Markers in NSCLC

One of the difficulties with treating NSCLC is its heterozygous nature **[12]**. The same tumor may have different cellular genetic profiles, thus responding to therapy differently. However there are some associated markers implicated in decreased survival in NSCLC including overexpressed or mutated Epidermal Growth Factor Receptor (EGFR), Anaplastic Lymphoma Kinase (ALK) gene rearrangements, loss of *p53* activity, and mutant *KRAS* **[12, 14]**. Many new biomarkers are under investigation; including proteins involved in cell proliferation and cell cycle. However, due to the heterogeneity of this cancer the prognostic value of these markers are variable. Currently *EGFR*, *ALK*, and *KRAS* gene statuses are tested in patients to determine therapeutic benefit.

Mutations in *KRAS* are among the most prevalent oncogene in lung cancer and occur in 32.2% of all NSCLC patients. Mutant *KRAS* is a marker of poor survival in patients with NSCLC **[15, 16]**. However, mutant *KRAS* does not seem to be a useful marker for prognostic value. A clinical study for patients with refractory NSCLC patients revealed that mutant *KRAS* was not associated with overall survival or progression-free survival. However, when distinct *KRAS* mutations are taken into account this is not entirely the case. Upon subsequent review, patients with G12C and G12V mutations had decreased progression-free survival compared to patients with other *KRAS* mutations or wild type *KRAS*. This was confirmed in a recent study which found patients with *KRAS G12C* had a higher tendency of recurrence and death as compared to other *KRAS* mutations or wild type *KRAS* **[15]**. Other retrospective studies have also shown that mutant *KRAS* does not seem to be a predictive marker for chemotherapy benefit. However, this may also be due to differences conferred by different *KRAS* mutations. Subtle changes in KRAS structure, dictated by each mutation, may directly affect substrate specificity. For example *KRAS* with a G12C mutation prefers to signal through Ras-related protein (RAL) whereas *KRAS* G12D prefers signaling through mitogen and extracellular signal-regulated kinase (MEK) **[17]**. However, patients with *KRAS* G12D may respond better to a MEK inhibitor than a patient with *KRAS* G12C (See section 1.4 for a more in depth description of KRAS signaling).

1.3.4 Therapy

Treatment choices for patients are based on the histopathology, stage of the cancer and age of the patient. For early stage cancers, lobectomies are the most common form of treatment and may be performed in conjunction with radiation, chemotherapy and/or targeted therapies [10]. Although much progress has been gained in cancer research (as reviewed in section 1.2.1) lung cancer is still the leading cause of cancer related death and there remains an immense need for new therapies.

1.3.4.1 Systemic Therapy

Systemic therapy can be through oral or intravenous chemotherapy. Currently patients with stage 0-IIIa will undergo a lobectomy to remove part or a whole lobe in hopes of removing the entire tumor. Stage Ia-IIIb will receive radiation therapy with or without chemotherapy [10]. Common chemotherapy drugs include platinum-based drugs like cisplatin, a DNA intercalator: taxol, a microtubule stabilizer; and gemcitabine, a drug which inhibits DNA synthesis. **Table 1.3** shows the suggested treatment schematic for patients at different stages [18].

1.3.4.2 Targeted Therapy

Patients with advanced disease (stage IV) also receive cytotoxic chemotherapy drugs, however if they test positive for certain markers, they will receive more targeted therapy. Crizotinib is a small molecule inhibitor that was originally developed for anaplastic large cell lymphoma, but recently has found success in treating the 5% of NSCLC patients with ALK fusions [19-21]. Patients with overexpressed EGFR receive inhibitors such as erlotinib or gefitinib. Several clinical trials have shown that patients with overexpressed EGFR treated with these inhibitors greatly benefit in terms of increased progression-free survival over traditional chemotherapy [19, 22, 23]. However EGFR inhibitors do not benefit patients with normal levels of EGFR. Although these inhibitors are initially successful at treated ALK or EGFR positive lung cancers, most patients become resistant to these therapies after 9-12 months [19, 24-26]. This is due to activating mutations in the kinase domains of both proteins, such as T790M in EGFR [14], which the drug is not effective at inhibiting therefore second generation drugs which overcome this setback are being sought.

Although there are no drugs to directly inhibit mutant *KRAS*, MEK, a downstream effector of KRAS signaling, has been shown to be a modest target. MEK inhibitors are not robust, likely due to the *KRAS* mutation status of the patient (Section 1.2.3.4) and suffer from increased cytotoxicity in normal cells (see section 3.2.1.2 for a more detailed discussion on MEK inhibitors). Thus there is a critical need for identification of druggable downstream targets of both EGFR/KRAS.

1.4 Mouse Models of Lung Cancer

To better study the factors involved in the initiation and progression of lung cancer, several murine models of lung cancer have been developed. Since the 1960s studies have been done to induce lung adenomas in mice via carcinogens. Common carcinogens used are urethane, and components of tobacco smoke, benxo(a)pyrene or 4-(methylnitrosamino)-1-(3-pyridyl)-1-butanone [27]. In spontaneous and chemically induced lung tumors, more than 90% of these tumors are driven by *Kras* mutations.

In 2001, two mutant *Kras* mouse models were made; the $Kras^{LA}$ and the $Kras^{LSL-G12D}$ mouse [28, 29]. Both models demonstrate that activation of mutant *Kras* predominately leads to adenocarcinoma, a subtype of NSCLC. The $Kras^{LA}$ mouse has a latent mutant *Kras* allele ($Kras^{G12D}$) which is activated through homologous recombination [28]. The mouse develops normally, but perishes at an early age due to high penetrance of early stage lesions. The second model, the $Kras^{LSL-G12D}$ mouse, enables conditional activation of mutant *Kras*. KRAS is necessary for embryonic development. In $Kras^{LSL-G12D}$ mice, one allele is wild type for *Kras* and the other includes an upstream synthetic stop flanked by lox-p sites which blocks the expression of a *Kras* mutated at codon 12 (glycine to aspartic acid) [29]. Mutant *Kras* is activated when Cre-recombinase is administered. Cre-recombinase recognizes the lox-p sites and removes the stop, allowing transcription to proceed. The titer of virus administered to this mouse directly correlates with the total of tumor burden, allowing control over the number of lesions. Other benefits include being able to monitor initiation as well as the different steps in tumor progression. This animal, however normally only occasionally will develop adenocarcinomas. Figure 1.3 is a schematic which shows the progression of tumorigenesis in this mouse. When the $Kras^{LSL-G12D}$ mouse is crossed with a *p53* null

(KP), after initiation of mutant *Kras*, these animals develop adenomas more quickly and also develop adenocarcinomas **[30, 31]**. Although this model better recapitulates the human disease, the rapid mortality of these mice makes it hard to monitor progression.

Other mouse models include ectopic xenograft models, in which human lung cancer cell lines are subcutaneously injected. Moreover, orthotopic models are also used which include mouse (syngeneic) or human cell lines are injected intravenously and mice subsequently develop primary and metastatic tumors. Overall, these models allow for quick analysis of tumor growth over time and as a result are useful for testing drug efficacy **[27]**. To date, these mouse models have been useful in elucidating new potential therapeutic targets, testing new antitumor agents, and providing new insights into the process of lung tumorigenesis.

1.5 EGFR/KRAS Signaling

1.5.1 EGFR

EGFR promotes cell proliferation through signaling cascades. EGFR is overexpressed in approximately 40-80% and mutated in 10% of NSCLC patients **[19, 32]**. Normal function of this receptor initiates when its ligand, Epidermal Growth Factor (EGF), binds to the extracellular domain of EGFR, causing EGFR to dimerize. Dimerization triggers auto-phosphorylation of its cytoplasmic kinase domains activating the receptor. Activated receptor primarily induces the KRAS/MAPK signaling cascades, resulting in cell cycle progression and cell proliferation (**Fig. 1.4**). Although, other pathways such as the PI3K/AKT and JNK/STAT are also activated leading to cell survival, migration, inflammation, increased transcription and proliferation [33]. However, the focus of this thesis will be primarily discussing the downstream KRAS/MAPK pathway.

1.5.2 KRAS

KRAS, a small GTPase, is activated by EGFR signaling when adaptor proteins recruit KRAS to the membrane in proximity to the receptor. KRAS farnesylation and palmitolyation (**Fig. 1.5)** helps facilitate association with the plasmid membrane once it is recruited **[34-37]**. These post-translational modifications are important for KRAS activation, and the enzymes that catalyze these reactions became potential targets of

inhibition. These inhibitors found success in tissue culture, but they failed in clinical trials **[34]**.

Guanine exchange factors (GEF), such as SOS **[38]**, mediate exchange of GDP for GTP on KRAS, also activating it. GTPase activating proteins (GAPs) facilitate hydrolysis of GTP to GDP to regulate this process, turning KRAS off (**Fig. 1.6**) **[34]**. *KRAS* mutations generally arise in the P-loop, a structure that controls whether the active site prefers GTP or GDP (G12 and G13) **[34]**. Some mutations, such as Q61, result in a constitutively active KRAS bound to GTP as the GAP is unable to hydrolyze GTP **[34]**. Activated KRAS stimulates the downstream kinase V-Raf Murine Sarcoma Viral Oncogene Homolog B1 (BRAF). BRAF activates mitogen and extracellular signal-regulated kinase (MEK) leading to cell cycle progression and proliferation (**Fig. 1.7**) **[34]**. As mentioned in section 1.2.3.4, specific mutations of *KRAS* may confer distinct specificity for downstream effectors as shown in **Figure 1.8.**

Although it is well documented that mitogenic signaling by EGFR/KRAS induces early cell cycle progression, the mechanism of how this signaling stimulates mitotic progression is unclear. KRAS activates MEK which phosphorylates ERK1/2. It is not known if ERK1/2 is phosphorylated in the cytoplasm or nucleus **[39]**, regardless phosphorylated ERK1/2 in the nucleus phosphorylates several transcription factors leading to expression of early cell cycle proteins such as Cyclin D1. It is known that EGFR/KRAS/MEK stimulates all stages of the cell cycle, although it is unclear how this pathway regulates later cell cycle events such as the G2 phase to transition to mitosis **[40, 41]**.

1.6 FADD

Another potential marker in lung cancer is Fas-associated death domain (FADD). FADD is an adaptor protein traditionally characterized in cell death pathways **[42-45]**. In recent years it has become apparent that FADD plays roles in other important cellular processes such as cell cycle progression and cell proliferation and has been implicated in different cancers, like lung cancer. However, the mechanism by which FADD modulates these pathways is not yet understood.

1.6.1 Chromosomal Location and Structure of FADD

FADD gene is located 11q13.3 on chromosome 11 and encodes 2 exons. FADD is a 23kDa adaptor protein containing two domains, a Death Domain (DD) and a Death Effector Domain (DED) (**Fig. 1.8**). FADD secondary structure is predominately alpha helices (**Fig. 1.9**) **[46]**. The first domain is a DD which interacts with DD containing cell death or inflammation related receptors such FAS or TRAIL **[42, 47, 48]**. The second domain is the DED which in interacts with pro-Caspase 8 and other proteins containing DED domains. FADD is expressed in all tissue and has been shown to be localized both in the cytoplasm and nucleus. FADD contains a nuclear localization and nuclear export sequence in its DED domain (**Fig. 1.8**). Exportin 5 has been shown to mediate FADD's transport into the nucleus **[49]**. It is now accepted that FADD's role in the nucleus is different than its role in the cytoplasm and will be described in the following sections.

1.6.2 Cell Death

FADD plays an important role in the extrinsic apoptosis pathway. FADD acts an adaptor, binding a death receptor's DD (such as the FAS receptor) with its own, causing a conformational change in FADD's DED. This conformational change allows pro-Caspase 8 to bind **[47, 48].** The complex of FADD, FAS receptor, and pro-Caspase 8 is known as the DISC complex. Pro-Caspase 8 oligomerizes then undergoes proteolytic cleavage of its pro domains to become active. Subsequently, activated Caspase 8 cleaves downstream Caspases, leading to the activation of Caspase 3 and ultimately cell death (**Fig. 1.9A**) **[47, 48]**. FADD has also been shown to initiate apoptosis independent of FAS, by oligomerizing with itself to form "death filaments" to which pro-Caspase 8 can bind initiating this pathway **[50, 51]**.

Necrosis is another form of cell death in which FADD plays an important role. FADD forms another complex with Caspase-8 and two kinases, Receptor-interacting serine/threonine-protein kinase 1 (RIPK1) and 3 (RIPK3) **[52]**. RIPK1 has a DD to which FADD binds. In a FAS or TRAIL receptor dependent manner, FADD forms a complex with Caspase 8, RIPK1and RIPK3 (**Fig. 1.9.B**). Caspase 8 activity regulates RIPK1 and RIPK3 by cleavage of their kinase domain and the cell undergoes apoptosis. When FADD is lost, Caspase 8 cannot inactivate RIPK1 and RIPK3. RIPK1 and RIPK3 can

then form a complex and phosphorylate each other to initiate necrosis (**Fig. 1.9C**) **[52]**. Interestingly, necrosis initiated by TNF occurs in a FADD independent manner **[52]**.

1.6.3 T-cell Proliferation

Although FADD has been well characterized as a protein important for cell death, it has roles outside of death and may positively regulate cell proliferation and cell cycle. Many reports describe the use of a dominant negative construct of FADD, where the DED is removed **[53-58]**. This construct inhibits FAS mediated apoptosis as well as causes a proliferation defect in MEFs and T-cells cultured from transgenic mice **[56]**. These mice had smaller thymus as well as lower numbers of thymocytes **[56]**. Mitogenic stimulation was also abrogated in these cells **[53, 56-59]**. It was postulated that the growth defect was not due to increased apoptosis, but that the cells were arrested or undergoing necroptosis **[60]**. It was later shown that FADD is post-translationally modified when mitogen stimuli were present, suggesting this modification was necessary for facilitating cell survival and growth **[61]**.

1.6.4 FADD Phosphorylation (Cell Cycle)

FADD is regulated by post-translational modifications. FADD is phosphorylated at Serine 194 (Serine 191 in mice) and this modification is associated with FADD's activity outside of cell death **[62-65]**. Phosphorylation of FADD does not affect FADD's ability to bind to the FAS receptor or impede cell death. However, this phosphorylation does affect FADD's location in the cell, which may affect FADD's role in cell death **[62, 66]**. Cells lacking FADD arrest in G2/M, suggesting FADD plays a role in cell cycle progression. When cells are arrested at G2/M with drugs that perturb microtubule formation (e.g. taxol or nocodozole), FADD is highly phosphorylated. Inhibition of the kinase which phosphorylates FADD leads to an increase in G2/M arrested cells, suggesting that FADD phosphorylation is also necessary for cells to progress through G2/M.

FADD is phosphorylated by several kinases: Casein Kinase 1alpha (CK1α), Polo-like Kinase 1 (PLK1), Aurora Kinase A (AURKA) and FIST/HIP kinase **[62, 64, 65, 67, 68]**. Both CK1α and PLK1 phosphorylate FADD at S194 (S191 in mouse) **[62, 68]**. AURKA phosphorylates FADD at S203; however the consequences of this modification are not quite known **[67]**. Recently, FADD has been shown to be dephosphorylated by

DUSP26, a nuclear phosphatase, and that this is regulated by AK2 **[69]**. Knockdown of AK2 caused a decrease in phosphorylation of FADD.

1.6.5 FADD in Cancer

The first indication that FADD had a role in cancer came in 2002 in a gene-expression profile of 86 primary lung adenocarcinoma samples **[70]**. *FADD* mRNA was demonstrated to be up-regulated and that this increases in mRNA correlated with increased protein level. This finding was confirmed by our group in 2005. We found that not only was FADD mRNA up-regulated in lung cancer patients, but this also correlated with poor survival **[71]**. It was later found that FADD is located on 11q13.3 on chromosome 11, which is highly amplified in lung cancer as well as head and neck cancer **[72]**. FADD phosphorylation is actually a more stringent indicator of survival in lung cancer and head and neck patients **[71-75]**. FADD phosphorylation also acts as a marker of proliferation in B-cell non-Hodgkin lymphomas **[76]**. Interestingly, our group also found *FADD* mRNA levels correlated with *KRAS* mutation status, suggesting a connection **[71]**.

Although FADD overexpression and phosphorylation is highly correlative with aggressive lung cancer and head and neck cancer, FADD appears to play a role as a tumor suppressor in cancers such as prostate and colon **[77-79]**. This may be due to FADD's roles in other signaling pathways which could be cell dependent. For example, in colon cancer inflammation plays a large role in tumorigenesis; loss of FADD would result in an increase in necrosis, potentially inflaming this cancer. This holds true in skin and colon mouse models. A loss of FADD resulted in massive activation of necrosis which resulted in cancer **[80, 81]**.

One of the goals of this thesis was to confirm a role of FADD in lung tumorigenesis.

1.7 CK1α

1.7.1 Chromosomal Location and Structure of CK1α

Casein Kinase 1 alpha (CK1α) is part of the Casein Kinase family of enzymes. It is a serine/threonine kinase which has been shown to regulate p53 and Wnt signaling. To date there are seven isoforms of CK1, α, β, ε, δ, γ1, γ2, and γ3 and two splice

variants of CK1α, CK1αS and CK1αL **[82]**. The *Csnk1a1* gene is located on chromosome 5 and codes for a 38kDa protein, which shares 50-70% homology with the other isoforms of CK1. CK1α has a shorter non-catalytic regulatory C terminus than all of the other isoforms **[82]**. Although no crystal structure has been solved for CK1α, there is for a structure of CK1δ. The CK1δ N terminus consists of 5 β-strands which with the α-helices of the C terminus forms the active site cleft. CK1α has a putative nuclear localization sequence (NLS), although only one of the CK1α variants has a complete NLS (CK1αL) **[83]**. The canonical substrate sequence is pSer/Thr-X-X-(X)-Ser/Thr, however sequences with several negatively charged amino acids or primed sequences, meaning another kinase has phosphorylated the substrate are suitable for CK1α **[84]**. CK1α is regulated through its localization as well as post-translational modifications, like neddylation and auto-phosphorylation **[82, 85]**. CK1α has been shown to be localized in the cytoplasm and in the nucleus on the centrosome and kinetochore **[62]**.

1.7.2 Wnt and p53 Signaling Regulation by CK1α

CK1α negatively regulates Wnt signaling. CK1α complexes with GSK3, APC, and Axin and together this complex acts to modify β-Catenin for degradation when Wnt ligand is absent. CK1α primes β-Catenin through phosphorylation at S45 for further phosphorylation by GSK3β and subsequent ubiquitination and degradation **[82, 84]**. When CK1α is depleted, β-Catenin is not phosphorylated and its levels stabilize and activation of the pathway occurs. Importantly, other CK1 isoforms also play a role in regulating Wnt signaling, suggesting that each isoform may redundantly modulate this pathway **[82, 86]**. In a model of colon cancer, loss of CK1α resulted in a massive increase in Wnt signaling. However, this activation did not result in tumorigenesis due to an increase in p53 levels and increased apoptosis **[87]**.

Loss of CK1α results in higher levels of p53 and this occurs through multiple pathways. First, CK1α negatively regulates p53 levels through modulation of MDMX or by physically interacting with MDM2. Phosphorylation of MDMX by CK1α causes stabilization of MDMX which results in decreased p53 levels. Second, CK1α promotes the MDMX-p53 complex as well **[88, 89]**. When CK1α is activity is impaired or CK1α is depleted or CK1α is depleted, MDMX is targeted for degradation and p53 levels increase.

1.7.3 FADD as a Substrate

As mentioned in section 1.5.4, FADD has been shown to be a substrate of CK1α. CK1α is likely the main kinase which regulates FADD's roles outside of apoptosis. As demonstrated by Alappat *et al.*, 2005 CK1α co-localizes with phosphorylated FADD at the mitotic spindle, and is responsible for FADD phosphorylation at S194 (S191 in mice) **[62]**. Inhibition of CK1α by inhibitors resulted in a decrease in phosphorylated FADD as well as cells arresting in G2/M **[62, 90, 91]**.

1.8 Conclusions

FADD mRNA and phosphorylated FADD levels have associated with poor outcome in patients with lung cancer as well as other cancers (Section 1.5.5). Increased *FADD* mRNA has been shown to correlate with *KRAS* mutation status, suggesting FADD may have a role in KRAS-mediated lung cancer. Inhibition of FADD phosphorylation through inhibiting its kinase may result in a new therapy for patients with mutant *KRAS* positive lung cancer. Because downstream KRAS mitogenesis signaling is not well understood we hypothesized that FADD has a role in facilitating KRAS-mediated mitogenic signaling. The goals of this thesis include: **1**. To determine if FADD is necessary for *Kras*-mediate lung oncogenesis in a mouse model of lung cancer; **2**. To determine if phosphorylation of FADD is necessary for *Kras*-mediated mitogenesis and cell proliferation in mouse embryonic fibroblasts (MEF); **3**. To determine if FADD is part of the RAS-MEK-ERK signaling pathway using MEF cells; **4**. To determine if CK1α has a role in *Kras*-mediated lung oncogenesis in a mouse model of lung cancer.

1.9 Figures

LUNGS

Trachea

Right Bronchus

Left Bronchus

Right Lobes

Left Lobes

Bronchioles
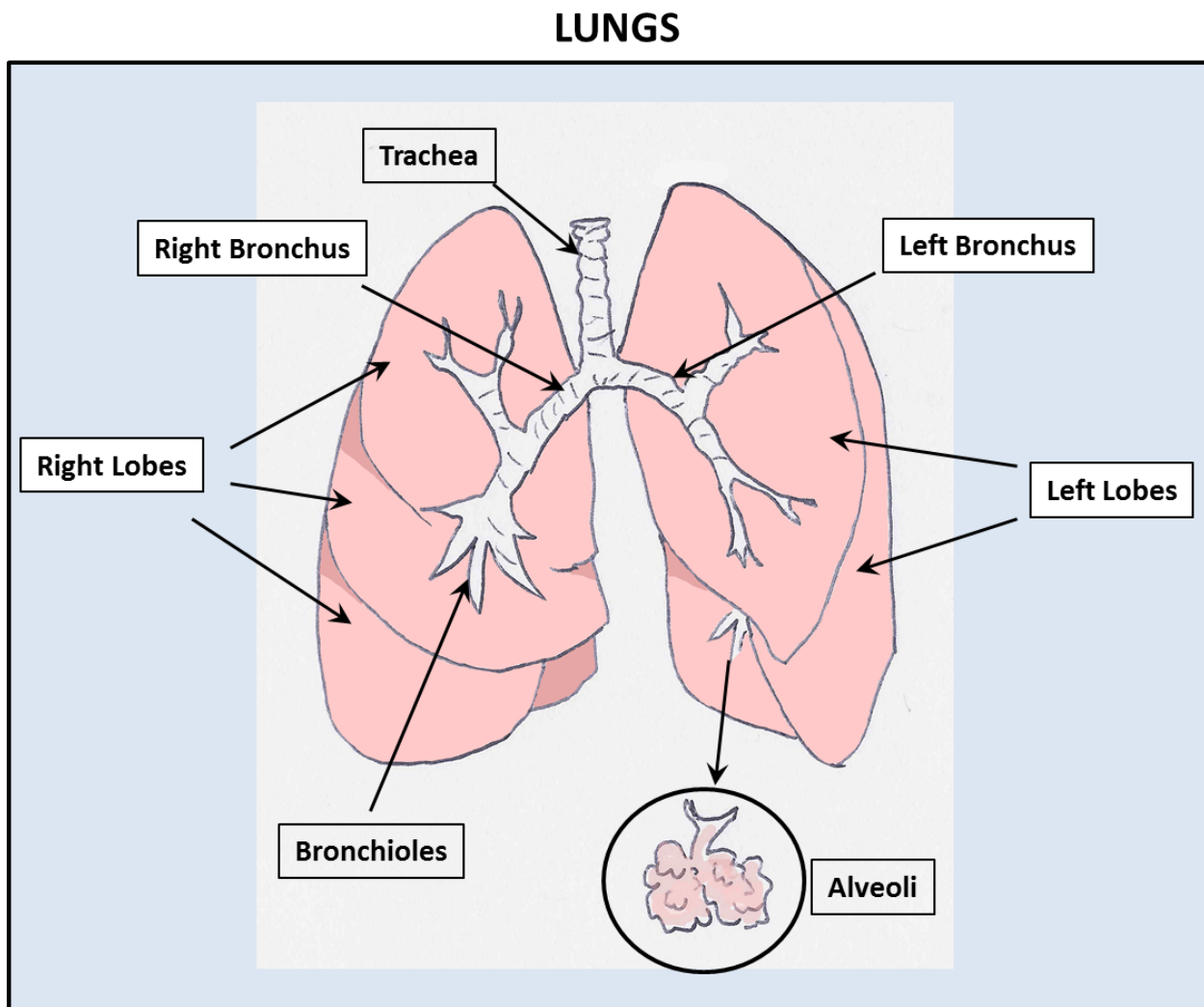
Alveoli

Figure 1.1 Schematic representation of the lung. The lung is composed of five lobes, three right and two left. Connecting these lobes are two bronchi which branch into smaller bronchioles which end at small sacs referred to the alveolar sac.
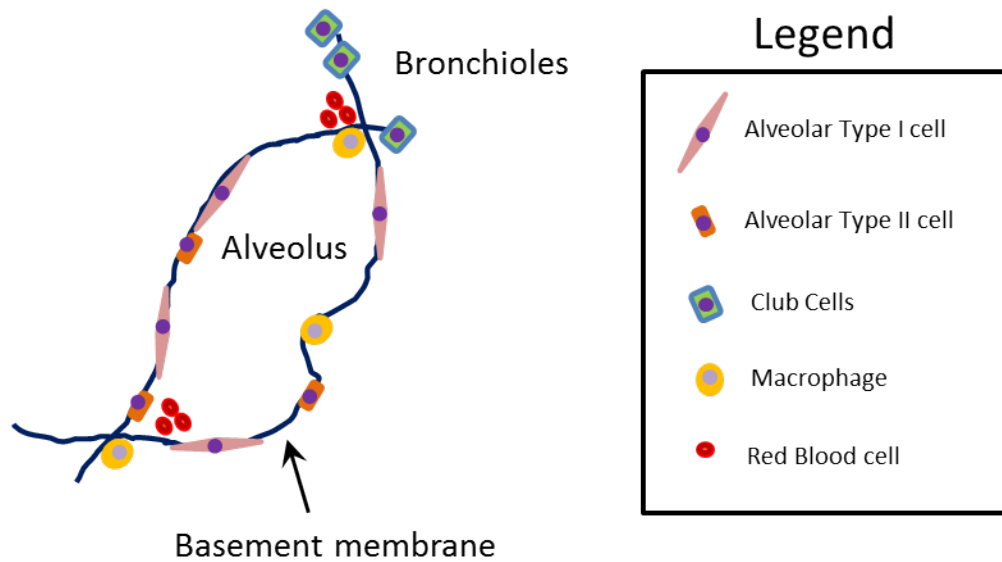
Figure 1.2 Schematic of the alveoli. The alveolar sac or alveolus is comprised of cells which facilitate gas exchange, type I cell and cells which produce surfactant, type II cell. Other cells which make up these structures are macrophages, fibroblasts and endothelial cells. The dark line represents the basement membrane which consists of both fibroblasts and endothelial cells.
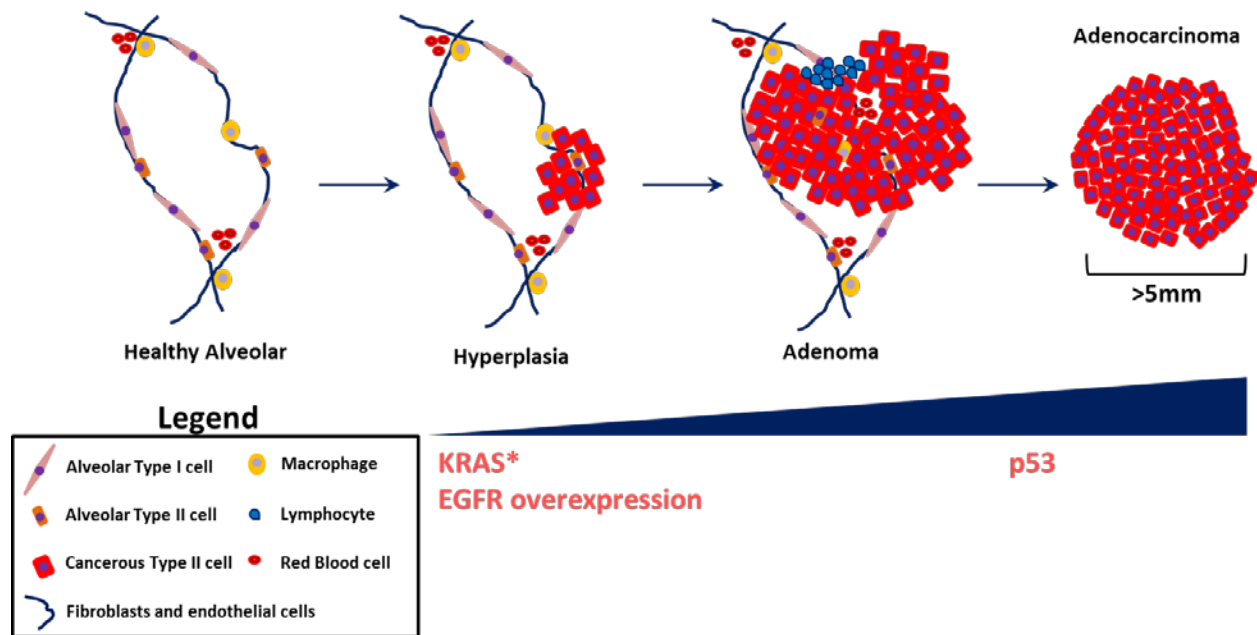
Figure 1.3 Schematic of hypothesized cancer progression of type II cells. Type II cells are thought to be the originators of adenocarcinoma in NSCLC. Overexpressed EGFR or mutant *KRAS* in these cells cause hyper-proliferation resulting in adenomas or cancer in situ in mouse models. Loss of p53 or additional mutations of other driver genes are necessary, in mouse models, for the regular occurrence of adenocarcinoma.
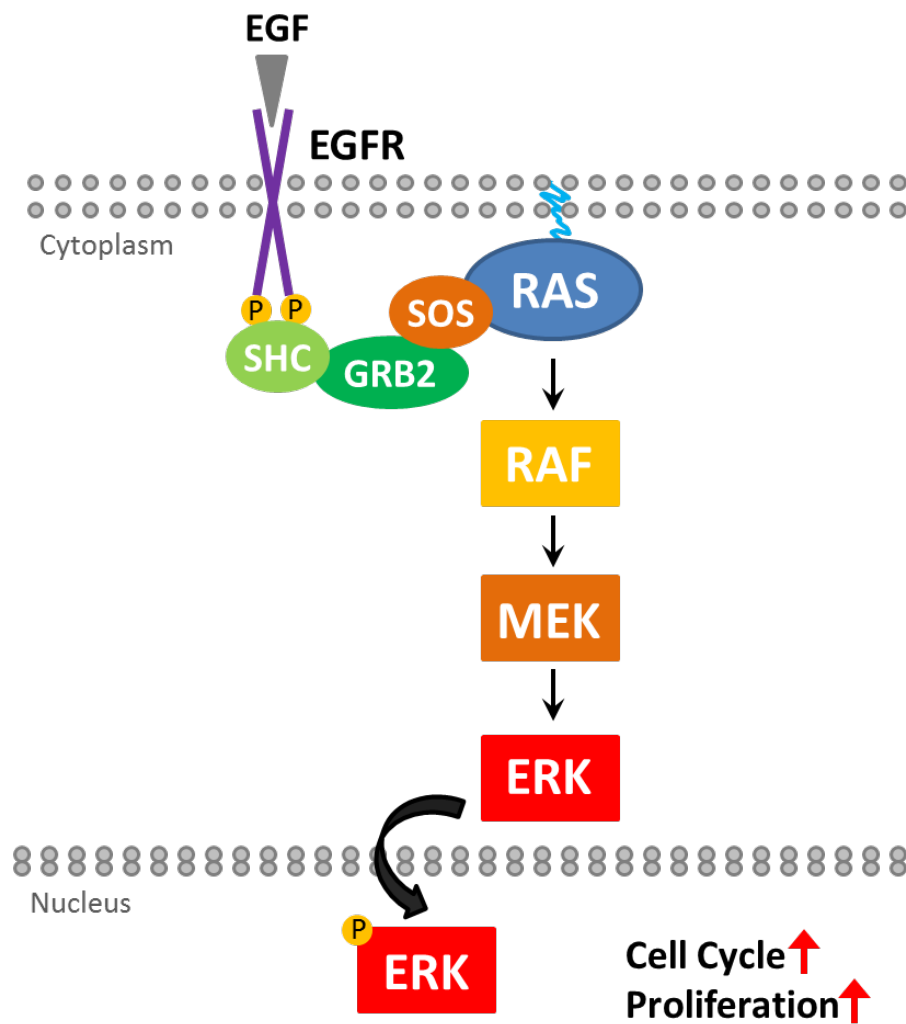
Figure 1.4 Diagram of the EGFR/KRAS pathway. Stimulation of the epidermal growth factor receptor (EGFR) primarily results in activation of the RAS/MAPK signaling cascade resulting in cell cycle progression and increased proliferation. **[34]**
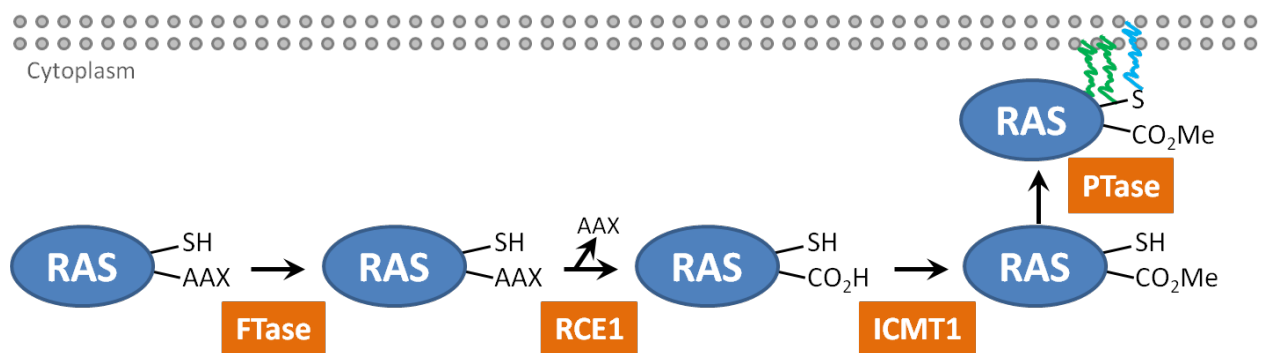
Figure 1.5 Post-translational modifications of RAS. RAS is farnesylated by FTase and palmitoylated by PTase enzymes. These modifications result in RAS associating with the plasma membrane and are necessary for RAS to facilitate activation of downstream pathways. **[34]**
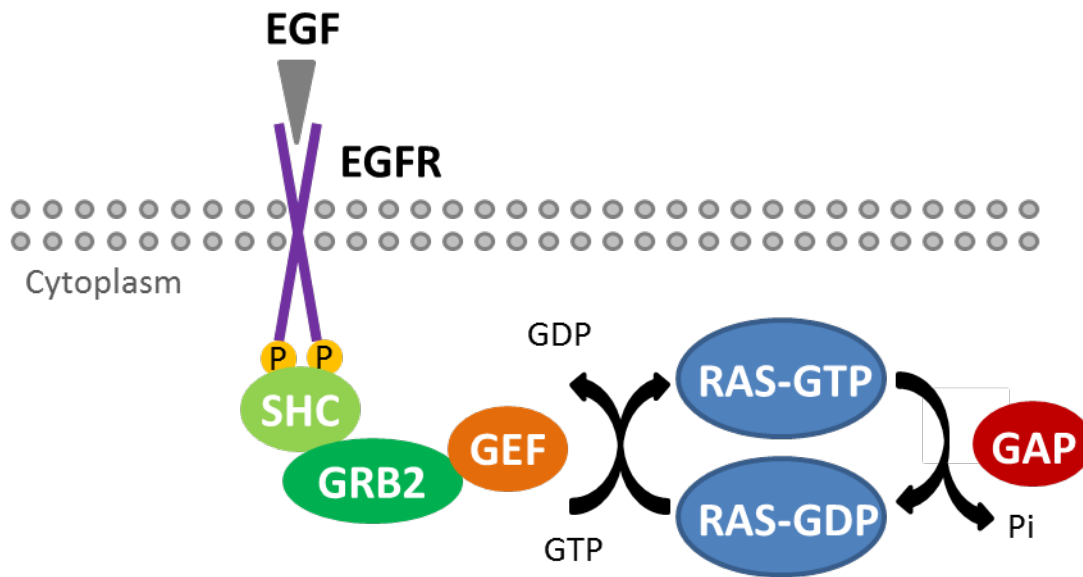
Figure 1.6 Diagram of the KRAS GAP/GEF cycle. RAS is activated when a GEF protein helps facilitate the diffusion of GDP from the nucleotide binding site, which allows GTP to bind. As a mechanism to shut off RAS, GAP proteins facilitate hydrolysis of the GTP to GDP+ Pi. Mutations in *RAS* result in an increased affinity for GTP as well as block GAP from acting on RAS. **[34]**
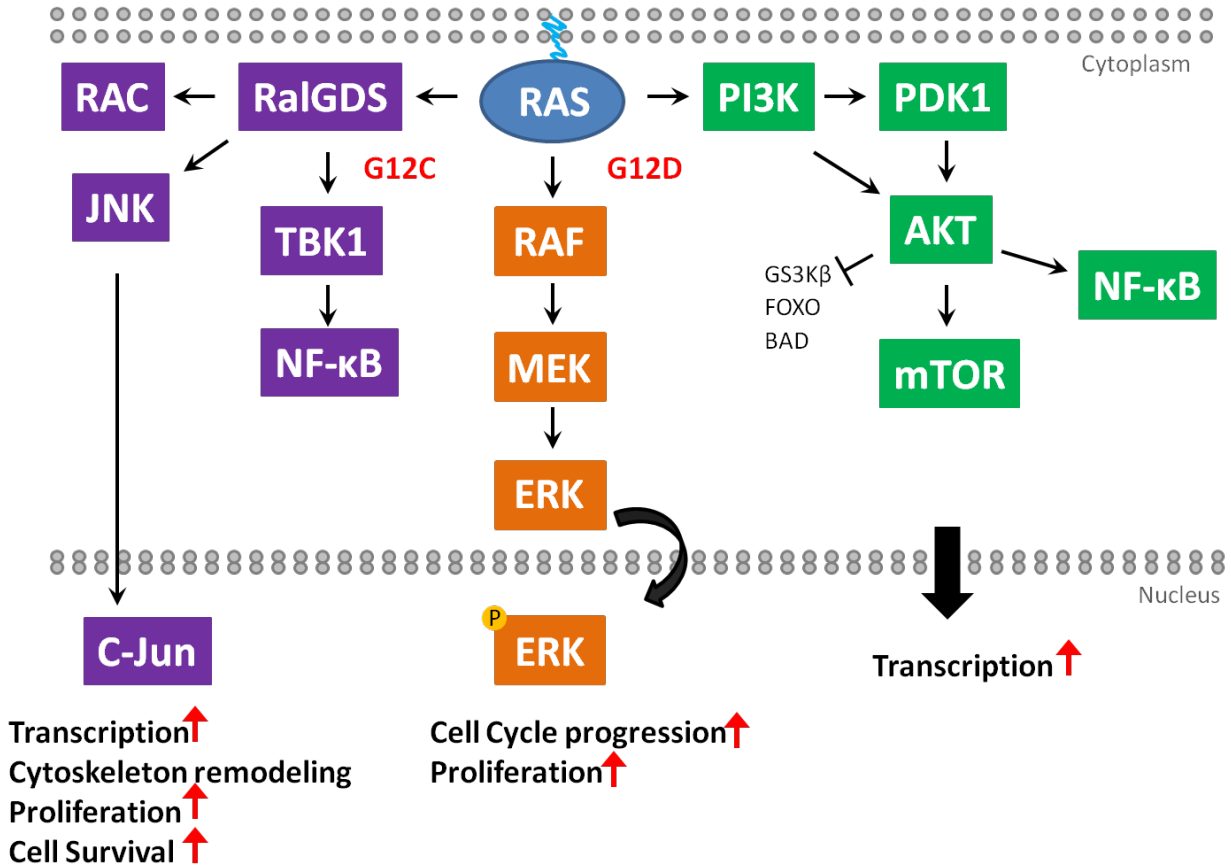
Figure 1.7 Schematic of the downstream pathways activated by RAS. RAS can signal through the PI3K/AKT, Ral and MAPK pathway. Each pathway regulates different cellular functions, all of which result in increased proliferation. Denoted in red are *KRAS* mutations associated with a downstream pathway. **[34]**
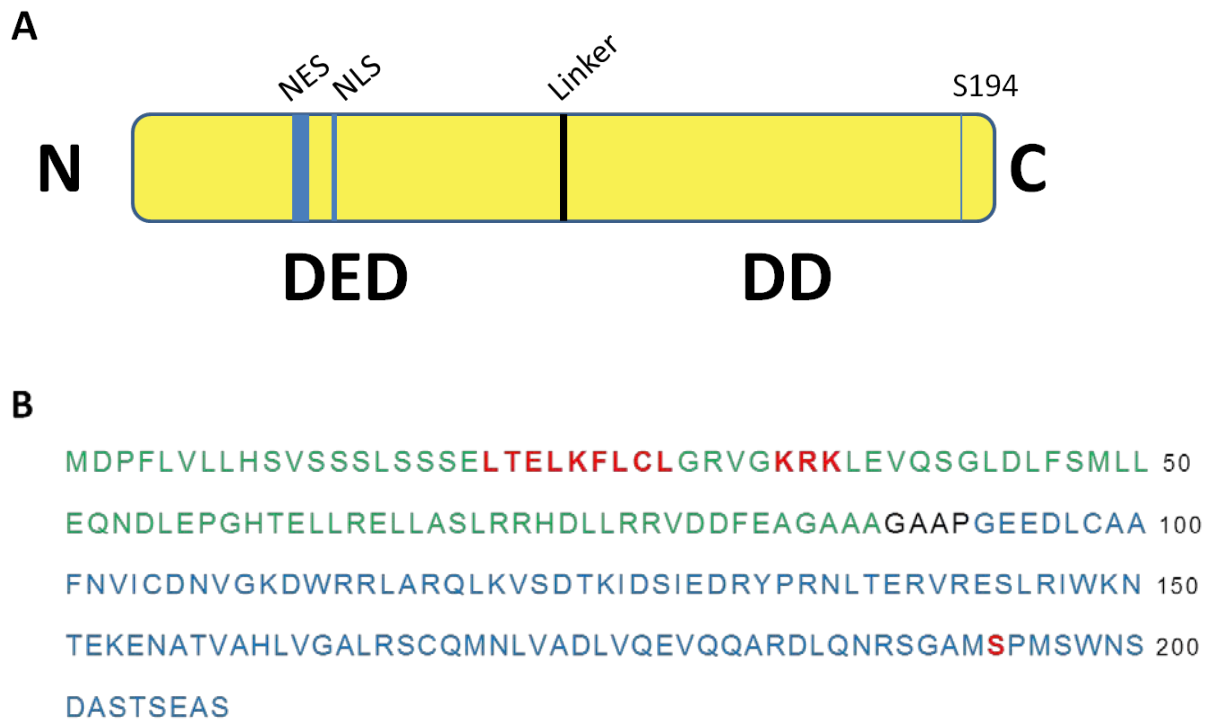
Figure 1.8 FADD Sequence. A). Schematic of human FADD showing the location of the DED and DD domains as well as the nuclear localization and nuclear exportation sequences. FADD is phosphorylated at Serine 194 in human FADD and Serine 191 in mouse FADD. B). Diagram showing the human FADD sequence, in which amino acids in green represent the DED and in blue are part of the DD. Amino acids in red are the NES, the NLS and the serine which is phosphorylated, respectively. **[92]**
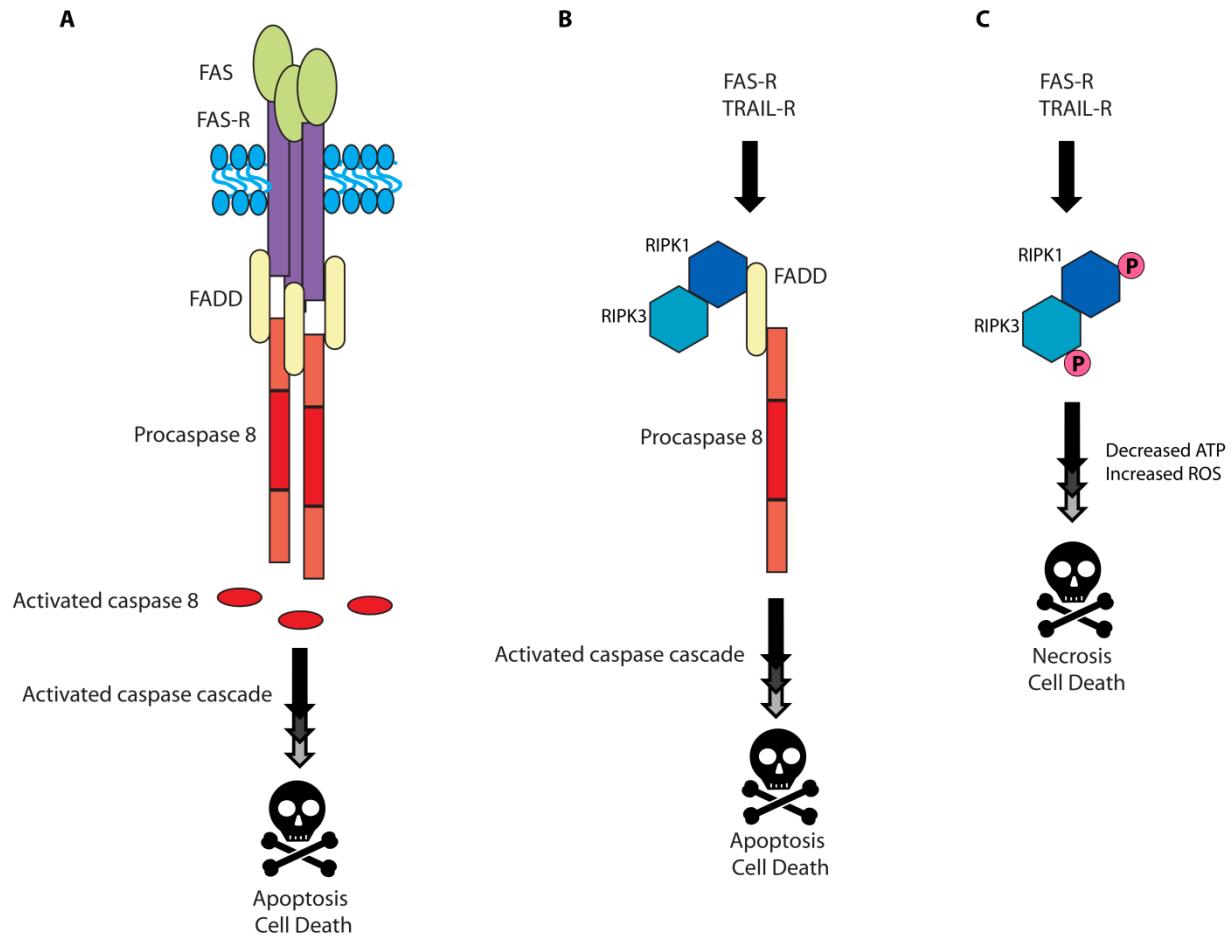
Figure 1.9 Diagram of FADD's role in cell death. A). FADD acts as an adaptor to facilitate receptor mediated cell death. FADD interacts with the FAS receptor via its DD and procaspase 8 with its DED. Upon binding FADD, procaspase 8 dimerizes and undergoes proteolytic cleavage of its pro domain. Activated Caspase 8 then initiates the Caspase cascade resulting in apoptosis. B) and C) illustrate FADD's role in RIPK mediated necrosis. FADD interacts with RIPK1 and procaspase 8. When FADD is present procaspase 8 activates itself and cleaves RIPK1 and RIPK3's kinase domain. When FADD is lost, RIPK1 and RIPK3 are not cleaved by procaspase 8. Both kinases then phosphorylate each other and signal necrosis. **[93]** and **[52].**

1.10 Tables

Table 1.1 Risk Factors

_____

- Smoking
- Exposure to Radon gas
- Exposure to Asbestos
- Exposure to Silica
- Exposure to Chromium
- Exposure to Nickel
- Exposure to Arsenic
- Exposure to Air pollution
- Family history of lung cancer
- Chest radiation

Table listing common environmental risk factors. Modified from **[5, 7]**

Table 1.2 TNM Staging

Stage	T	N	M
Occult	TX	N0	M0
Stage 0	Tis	N0	M0
	T1a	N0	M0
Stage IA	T1b	N0	M0
Stage IB	T2a	N0	M0
	T2b	N0	M0
	T1a	N1	M0
	T1b	N1	M0
Stage IIA	T2a	N1	M0
	T2b	N1	M0
Stage IIB	T3	N0	M0
	T1a	N2	M0
	T1b	N2	M0
	T2a	N2	M0
	T2b	N2	M0
	T3	N1	M0
	T3	N2	M0
	T4	N0	M0
Stage IIIA	T4	N1	M0
	T1a	N3	M0
	T1b	N3	M0
	T2a	N3	M0
	T2b	N3	M0
	T3	N3	M0
	T4	N2	M0
Stage IIIB	T4	N3	M0
	Any T	Any N	M1a
Stage IV	Any T	Any N	M1b

Modified from **[13].** **T** refers to tumor, **N** to lymph node and **M** represents metastasis.

Table 1.3 Treatments by Stage

Stage (TNM Staging Criteria)		Standard Treatment Options
Occult NSCLC		Surgery
Stage 0 NSCLC		Surgery
		Endobronchial therapies
Stages IA and IB NSCLC		Surgery
		Radiation therapy
Stages IIA and IIB NSCLC		Surgery
		Neoadjuvant chemotherapy
		Adjuvant chemotherapy
		Radiation therapy
Stage IIIA NSCLC	Resected or resectable disease	Surgery
		Neoadjuvant therapy
		Adjuvant therapy
	Unresectable disease	Radiation therapy
		Chemoradiation therapy
	Superior sulcus tumors	Radiation therapy alone
		Radiation therapy and surgery
		Concurrent chemotherapy with radiation therapy and surgery
		Surgery alone (for selected patients)
	Tumors that invade the chest wall	Surgery
		Surgery and radiation therapy
		Radiation therapy alone
		Chemotherapy combined with radiation therapy and/or surgery
Stage IIIB NSCLC		Sequential or concurrent chemotherapy and radiation therapy
		Chemotherapy followed by surgery (for selected patients)
		Radiation therapy alone

Stage (<u>TNM Staging Criteria</u>)	Standard Treatment Options
Stage IV NSCLC	Cytotoxic combination chemotherapy (first line)
	Combination chemotherapy with bevacizumab or cetuximab
	EGFR tyrosine kinase inhibitors (first line)
	EML4-ALK inhibitors in patients with EML-ALK translocations
	Maintenance therapy following first-line chemotherapy
	Endobronchial laser therapy and/or brachytherapy (for obstructing lesions)
	External-beam radiation therapy (primarily for palliation of local symptomatic tumor growth)
Recurrent NSCLC	Radiation therapy (for palliation)
	Chemotherapy or kinase inhibitors alone
	EGFR inhibitors in patients with/without EGFR mutations
	EML4-ALK inhibitors in patients with EML-ALK translocations
	Surgical resection of isolated cerebral metastasis (for highly selected patients)
	Laser therapy or interstitial radiation therapy (for endobronchial lesions)
	Stereotactic radiation surgery (for highly selected patients)

Modified from **[18]**

1.11 References

1.   Herzog, E.L., et al., *Knowns and unknowns of the alveolus.* Proc Am Thorac Soc, 2008. **5**(7): p. 778-82.

2.   Mason, R.J., *Biology of alveolar type II cells.* Respirology, 2006. **11 Suppl**: p. S12-5.

3.   Crapo, J.D., et al., *Cell number and cell characteristics of the normal human lung.* Am Rev Respir Dis, 1982. **126**(2): p. 332-7.

4.   Andreeva, A.V., M.A. Kutuzov, and T.A. Voyno-Yasenetskaya, *Regulation of surfactant secretion in alveolar type II cells.* Am J Physiol Lung Cell Mol Physiol, 2007. **293**(2): p. L259-71.

5.   Ridge, C.A., A.M. McErlean, and M.S. Ginsberg, *Epidemiology of lung cancer.* Semin Intervent Radiol, 2013. **30**(2): p. 93-8.

6.   Rivera, M.P., *Lung cancer in women: differences in epidemiology, biology, histology, and treatment outcomes.* Semin Respir Crit Care Med, 2013. **34**(6): p. 792-801.

7.   Pallis, A.G. and K.N. Syrigos, *Lung cancer in never smokers: disease characteristics and risk factors.* Crit Rev Oncol Hematol, 2013. **88**(3): p. 494-503.

8.   Thomas, J.L., et al., *Metabolites of a tobacco-specific lung carcinogen in children exposed to secondhand or thirdhand tobacco smoke in their homes.* Cancer Epidemiol Biomarkers Prev, 2011. **20**(6): p. 1213-21.

9.   Vineis, P., et al., *Tobacco and cancer: recent epidemiological evidence.* J Natl Cancer Inst, 2004. **96**(2): p. 99-106.

10.   Johnson, D.H., J.H. Schiller, and P.A. Bunn, Jr., *Recent clinical advances in lung cancer management.* J Clin Oncol, 2014. **32**(10): p. 973-82.

11.   Blanchon, F., et al., *4-year mortality in patients with non-small-cell lung cancer: development and validation of a prognostic index.* Lancet Oncol, 2006. **7**(10): p. 829-36.

12.   Chen, Z., et al., *Non-small-cell lung cancers: a heterogeneous set of diseases.* Nat Rev Cancer, 2014. **14**(8): p. 535-46.

13.   Mirsadraee, S., et al., *The 7th lung cancer TNM classification and staging system: Review of the changes and implications.* World J Radiol, 2012. **4**(4): p. 128-34.

14.   Herbst, R.S., J.V. Heymach, and S.M. Lippman, *Lung cancer.* N Engl J Med, 2008. **359**(13): p. 1367-80.

15.   Nadal, E., et al., *KRAS-G12C Mutation Is Associated with Poor Outcome in Surgically Resected Lung Adenocarcinoma.* J Thorac Oncol, 2014.

16.   Meng, D., et al., *Prognostic value of K-RAS mutations in patients with non-small cell lung cancer: a systematic review with meta-analysis.* Lung Cancer, 2013. **81**(1): p. 1-10.

17.   Ihle, N.T., et al., *Effect of KRAS oncogene substitutions on protein behavior: implications for signaling and clinical outcome.* J Natl Cancer Inst, 2012. **104**(3): p. 228-39.

18.   www.cancer.gov.

19.   Nguyen, K.S., J.W. Neal, and H. Wakelee, *Review of the current targeted therapies for non-small-cell lung cancer.* World J Clin Oncol, 2014. **5**(4): p. 576-87.

20.   Christensen, J.G., et al., *Cytoreductive antitumor activity of PF-2341066, a novel inhibitor of anaplastic lymphoma kinase and c-Met, in experimental models of anaplastic large-cell lymphoma.* Mol Cancer Ther, 2007. **6**(12 Pt 1): p. 3314-22.

21.   Shaw, A.T., et al., *Crizotinib versus chemotherapy in advanced ALK-positive lung cancer.* N Engl J Med, 2013. **368**(25): p. 2385-94.

22.   Zhou, C., et al., *Erlotinib versus chemotherapy as first-line treatment for patients with advanced EGFR mutation-positive non-small-cell lung cancer (OPTIMAL, CTONG-0802): a multicentre, open-label, randomised, phase 3 study.* Lancet Oncol, 2011. **12**(8): p. 735-42.

23.   Rosell, R., et al., *Erlotinib versus standard chemotherapy as first-line treatment for European patients with advanced EGFR mutation-positive non-small-cell lung cancer (EURTAC): a multicentre, open-label, randomised phase 3 trial.* Lancet Oncol, 2012. **13**(3): p. 239-46.

24.   Kobayashi, S., et al., *EGFR mutation and resistance of non-small-cell lung cancer to gefitinib.* N Engl J Med, 2005. **352**(8): p. 786-92.

25.   Kobayashi, S., et al., *An alternative inhibitor overcomes resistance caused by a mutation of the epidermal growth factor receptor.* Cancer Res, 2005. **65**(16): p. 7096-101.

26.   Pao, W., et al., *Acquired resistance of lung adenocarcinomas to gefitinib or erlotinib is associated with a second mutation in the EGFR kinase domain.* PLoS Med, 2005. **2**(3): p. e73.

27.   de Seranno, S. and R. Meuwissen, *Progress and applications of mouse models for human lung cancer.* Eur Respir J, 2010. **35**(2): p. 426-43.

28.   Johnson, L., et al., *Somatic activation of the K-ras oncogene causes early onset lung cancer in mice.* Nature, 2001. **410**(6832): p. 1111-6.

29.   Jackson, E.L., et al., *Analysis of lung tumor initiation and progression using conditional expression of oncogenic K-ras.* Genes Dev, 2001. **15**(24): p. 3243-8.

30.   Jackson, E.L., et al., *The differential effects of mutant p53 alleles on advanced murine lung cancer.* Cancer Res, 2005. **65**(22): p. 10280-8.

31.   DuPage, M., A.L. Dooley, and T. Jacks, *Conditional mouse lung cancer models using adenoviral or lentiviral delivery of Cre recombinase.* Nat Protoc, 2009. **4**(7): p. 1064-72.

32.   Roberts, P.J. and C.J. Der, *Targeting the Raf-MEK-ERK mitogen-activated protein kinase cascade for the treatment of cancer.* Oncogene, 2007. **26**(22): p. 3291-310.

33.   Henson, E.S. and S.B. Gibson, *Surviving cell death through epidermal growth factor (EGF) signal transduction pathways: implications for cancer therapy.* Cell Signal, 2006. **18**(12): p. 2089-97.

34.   Wang, Y., et al., *Targeting mutant KRAS for anticancer therapeutics: a review of novel small molecule modulators.* J Med Chem, 2013. **56**(13): p. 5219-30.

35.   Casey, P.J., et al., *p21ras is modified by a farnesyl isoprenoid.* Proc Natl Acad Sci U S A, 1989. **86**(21): p. 8323-7.

36.   Hancock, J.F., et al., *All ras proteins are polyisoprenylated but only some are palmitoylated.* Cell, 1989. **57**(7): p. 1167-77.

37.   Hancock, J.F., H. Paterson, and C.J. Marshall, *A polybasic domain or palmitoylation is required in addition to the CAAX motif to localize p21ras to the plasma membrane.* Cell, 1990. **63**(1): p. 133-9.

38.   Quilliam, L.A., et al., *Membrane-targeting potentiates guanine nucleotide exchange factor CDC25 and SOS1 activation of Ras transforming activity.* Proc Natl Acad Sci U S A, 1994. **91**(18): p. 8512-6.

39.   Roskoski, R., Jr., *ERK1/2 MAP kinases: structure, function, and regulation.* Pharmacol Res, 2012. **66**(2): p. 105-43.

40.   Meloche, S. and J. Pouyssegur, *The ERK1/2 mitogen-activated protein kinase pathway as a master regulator of the G1- to S-phase transition.* Oncogene, 2007. **26**(22): p. 3227-39.

41.   Liu, X., et al., *The MAP kinase pathway is required for entry into mitosis and cell survival.* Oncogene, 2004. **23**(3): p. 763-76.

42.   Boldin, M.P., et al., *A novel protein that interacts with the death domain of Fas/APO1 contains a sequence motif related to the death domain.* J Biol Chem, 1995. **270**(14): p. 7795-8.

43.   Strasser, A. and K. Newton, *FADD/MORT1, a signal transducer that can promote cell death or cell growth.* Int J Biochem Cell Biol, 1999. **31**(5): p. 533-7.

44.   Chinnaiyan, A.M., et al., *FADD, a novel death domain-containing protein, interacts with the death domain of Fas and initiates apoptosis.* Cell, 1995. **81**(4): p. 505-12.

45.   Zhang, J. and A. Winoto, *A mouse Fas-associated protein with homology to the human Mort1/FADD protein is essential for Fas-induced apoptosis.* Mol Cell Biol, 1996. **16**(6): p. 2756-63.

46.   Carrington, P.E., et al., *The structure of FADD and its mode of interaction with procaspase-8.* Mol Cell, 2006. **22**(5): p. 599-610.

47.   Chaudhary, P.M., et al., *Death receptor 5, a new member of the TNFR family, and DR4 induce FADD-dependent apoptosis and activate the NF-kappaB pathway.* Immunity, 1997. **7**(6): p. 821-30.

48.   Schneider, P., et al., *TRAIL receptors 1 (DR4) and 2 (DR5) signal FADD-dependent apoptosis and activate NF-kappaB.* Immunity, 1997. **7**(6): p. 831-6.

49.   Screaton, R.A., et al., *Fas-associated death domain protein interacts with methyl-CpG binding domain protein 4: a potential link between genome surveillance and apoptosis.* Proc Natl Acad Sci U S A, 2003. **100**(9): p. 5211-6.

50.   Wang, S., et al., *Detection of Fas-associated death domain and its variants' self-association by fluorescence resonance energy transfer in living cells.* Mol Imaging, 2013. **12**(2): p. 111-20.

51.   Siegel, R.M., et al., *Death-effector filaments: novel cytoplasmic structures that recruit caspases and trigger apoptosis.* J Cell Biol, 1998. **141**(5): p. 1243-53.

52.   Moquin, D. and F.K. Chan, *The molecular regulation of programmed necrotic cell injury.* Trends Biochem Sci, 2010. **35**(8): p. 434-41.

53.   Newton, K., et al., *A dominant interfering mutant of FADD/MORT1 enhances deletion of autoreactive thymocytes and inhibits proliferation of mature T lymphocytes.* EMBO J, 1998. **17**(3): p. 706-18.

54.   Newton, K., et al., *Effects of a dominant interfering mutant of FADD on signal transduction in activated T cells.* Curr Biol, 2001. **11**(4): p. 273-6.

55.   Hueber, A.O., et al., *A dominant negative Fas-associated death domain protein mutant inhibits proliferation and leads to impaired calcium mobilization in both T-cells and fibroblasts.* J Biol Chem, 2000. **275**(14): p. 10453-62.

56.   Walsh, C.M., et al., *A role for FADD in T cell activation and development.* Immunity, 1998. **8**(4): p. 439-49.

57.   Newton, K., A.W. Harris, and A. Strasser, *FADD/MORT1 regulates the pre-TCR checkpoint and can function as a tumour suppressor.* EMBO J, 2000. **19**(5): p. 931-41.

58.   Zornig, M., A.O. Hueber, and G. Evan, *p53-dependent impairment of T-cell proliferation in FADD dominant-negative transgenic mice.* Curr Biol, 1998. **8**(8): p. 467-70.

59.   Zhang, J., et al., *Fas-mediated apoptosis and activation-induced T-cell proliferation are defective in mice lacking FADD/Mort1.* Nature, 1998. **392**(6673): p. 296-300.

60.   Osborn, S.L., et al., *Fas-associated death domain (FADD) is a negative regulator of T-cell receptor-mediated necroptosis.* Proc Natl Acad Sci U S A, 2010. **107**(29): p. 13034-9.

61.   O'Reilly, L.A., et al., *Modifications and intracellular trafficking of FADD/MORT1 and caspase-8 after stimulation of T lymphocytes.* Cell Death Differ, 2004. **11**(7): p. 724-36.

62.   Alappat, E.C., et al., *Phosphorylation of FADD at serine 194 by CKIalpha regulates its nonapoptotic activities.* Mol Cell, 2005. **19**(3): p. 321-32.

63.   Kennedy, N.J. and R.C. Budd, *Phosphorylation of FADD/MORT1 and Fas by kinases that associate with the membrane-proximal cytoplasmic domain of Fas.* J Immunol, 1998. **160**(10): p. 4881-8.

64.   Rochat-Steiner, V., et al., *FIST/HIPK3: a Fas/FADD-interacting serine/threonine kinase that induces FADD phosphorylation and inhibits fas-mediated Jun NH(2)-terminal kinase activation.* J Exp Med, 2000. **192**(8): p. 1165-74.

65.   Scaffidi, C., et al., *Phosphorylation of FADD/ MORT1 at serine 194 and association with a 70-kDa cell cycle-regulated protein kinase.* J Immunol, 2000. **164**(3): p. 1236-42.

66.   Bhojani, M.S., et al., *Nuclear localized phosphorylated FADD induces cell proliferation and is associated with aggressive lung cancer.* Cell Cycle, 2005. **4**(11): p. 1478-81.

67.   Jang, M.S., et al., *Cooperative phosphorylation of FADD by Aur-A and Plk1 in response to taxol triggers both apoptotic and necrotic cell death.* Cancer Res, 2011. **71**(23): p. 7207-15.

68.   Jang, M.S., et al., *Phosphorylation by polo-like kinase 1 induces the tumor-suppressing activity of FADD.* Oncogene, 2011. **30**(4): p. 471-81.

69.   Kim, H., et al., *The DUSP26 phosphatase activator adenylate kinase 2 regulates FADD phosphorylation and cell growth.* Nat Commun, 2014. **5**: p. 3351.

70.   Beer, D.G., et al., *Gene-expression profiles predict survival of patients with lung adenocarcinoma.* Nat Med, 2002. **8**(8): p. 816-24.

71.   Chen, G., et al., *Phosphorylated FADD induces NF-kappaB, perturbs cell cycle, and is associated with poor outcome in lung adenocarcinomas.* Proc Natl Acad Sci U S A, 2005. **102**(35): p. 12507-12.

72.   Gibcus, J.H., et al., *Amplicon mapping and expression profiling identify the Fas-associated death domain gene as a new driver in the 11q13.3 amplicon in laryngeal/pharyngeal cancer.* Clin Cancer Res, 2007. **13**(21): p. 6257-66.

73.   Rasamny, J.J., et al., *Cyclin D1 and FADD as biomarkers in head and neck squamous cell carcinoma.* Otolaryngol Head Neck Surg, 2012. **146**(6): p. 923-31.

74.   Fan, S., et al., *Prognostic impact of Fas-associated death domain, a key component in death receptor signaling, is dependent on the presence of lymph node metastasis in head and neck squamous cell carcinoma.* Cancer Biol Ther, 2013. **14**(4): p. 365-9.

75.   Schrijvers, M.L., et al., *FADD expression as a prognosticator in early-stage glottic squamous cell carcinoma of the larynx treated primarily with radiotherapy.* Int J Radiat Oncol Biol Phys, 2012. **83**(4): p. 1220-6.

76.   Drakos, E., et al., *Expression of serine 194-phosphorylated Fas-associated death domain protein correlates with proliferation in B-cell non-Hodgkin lymphomas.* Hum Pathol, 2011. **42**(8): p. 1117-24.

77.   Wang, Q.R., et al., *Apigenin suppresses the growth of colorectal cancer xenografts via phosphorylation and up-regulated FADD expression.* Oncol Lett, 2011. **2**(1): p. 43-47.

78.   Shimada, K., et al., *Phosphorylation of Fas-associated death domain contributes to enhancement of etoposide-induced apoptosis in prostate cancer cells.* Jpn J Cancer Res, 2002. **93**(10): p. 1164-74.

79.   Ikeda, T., et al., *Phosphorylation status of Fas-associated death domain protein is associated with biochemical recurrence after radical prostatectomy.* Urology, 2013. **81**(3): p. 607-10.

80.   Bonnet, M.C., et al., *The adaptor protein FADD protects epidermal keratinocytes from necroptosis in vivo and prevents skin inflammation.* Immunity, 2011. **35**(4): p. 572-82.

81.   Welz, P.S., et al., *FADD prevents RIP3-mediated epithelial cell necrosis and chronic intestinal inflammation.* Nature, 2011. **477**(7364): p. 330-4.

82.   Knippschild, U., et al., *The CK1 Family: Contribution to Cellular Stress Response and Its Role in Carcinogenesis.* Front Oncol, 2014. **4**: p. 96.

83.   Burzio, V., et al., *Biochemical and cellular characteristics of the four splice variants of protein kinase CK1alpha from zebrafish (Danio rerio).* J Cell Biochem, 2002. **86**(4): p. 805-14.

84.   Marin, O., et al., *A noncanonical sequence phosphorylated by casein kinase 1 in beta-catenin may play a role in casein kinase 1 targeting of important signaling proteins.* Proc Natl Acad Sci U S A, 2003. **100**(18): p. 10193-200.

85.   Budini, M., et al., *Autophosphorylation of carboxy-terminal residues inhibits the activity of protein kinase CK1alpha.* J Cell Biochem, 2009. **106**(3): p. 399-408.

86.   Umar, S., et al., *Dual alterations in casein kinase I-epsilon and GSK-3beta modulate beta-catenin stability in hyperproliferating colonic epithelia.* Am J Physiol Gastrointest Liver Physiol, 2007. **292**(2): p. G599-607.

87.   Elyada, E., et al., *CKIalpha ablation highlights a critical role for p53 in invasiveness control.* Nature, 2011. **470**(7334): p. 409-13.

88.   Chen, L., et al., *Regulation of p53-MDMX interaction by casein kinase 1 alpha.* Mol Cell Biol, 2005. **25**(15): p. 6509-20.

89.   Wu, S., et al., *Casein kinase 1alpha regulates an MDMX intramolecular interaction to stimulate p53 binding.* Mol Cell Biol, 2012. **32**(23): p. 4821-32.

90.   Schinske, K.A., et al., *A novel kinase inhibitor of FADD phosphorylation chemosensitizes through the inhibition of NF-kappaB.* Mol Cancer Ther, 2011. **10**(10): p. 1807-17.

91.   Khan, A.P., et al., *High-throughput molecular imaging for the identification of FADD kinase inhibitors.* J Biomol Screen, 2010. **15**(9): p. 1063-70.

92.   Gomez-Angelats, M. and J.A. Cidlowski, *Molecular evidence for the nuclear localization of FADD.* Cell Death Differ, 2003. **10**(7): p. 791-7.

93.   Lee, E.W., et al., *The roles of FADD in extrinsic apoptosis and necroptosis.* BMB Rep, 2012. **45**(9): p. 496-508.

CHAPTER 2

THE ROLE OF FAS ASSOCIATED DEATH DOMAIN IN *KRAS*-MEDIATED LUNG ONCOGENESIS

2.1 Abstract

Although genomic amplification and phosphorylation of Fas-Associated Death Domain (FADD) has been associated with poor clinical outcome in lung and head and neck cancer, its role in oncogenesis is not fully understood. Here, we describe the requirement for FADD in lung oncogenesis by utilizing conditional murine models of *Kras*-driven lung cancer. In the absence of FADD, abrogation of tumor growth was observed wherein a lower proliferative index and decreased activation of downstream effectors of the RAS-mitogen-activated protein kinase (MAPK) pathway, including phosphorylated extracellular signal-regulated kinase 1 and 2 (pERK1/2), phosphorylated retinoblastoma (pRB) and Cyclin D1, indicated alterations in cell cycle progression. Studies using embryonic fibroblasts revealed that the induction of mitogenesis upon activation of the RAS-MAPK pathway required FADD and its phosphorylation by Casein Kinase 1 alpha (CK1α). A conditional mouse wherein CK1α expression was ablated simultaneous with *Kras* activation confirmed a requirement for FADD-phosphorylation in *Kras*-mediated lung oncogenesis. Phosphorylation of FADD during G2/M and its interaction with mediators of the G2/M transition, including Polo-Like Kinase 1 (PLK1), Aurora Kinase A (AURKA) and Budding Uninhibited by Benzimidazoles 1 (BUB1), provide a molecular basis for a requirement of FADD and its phosphorylation in *Kras*-mediated mitogenesis and demonstrate CK1α as a therapeutic target for *Kras*-driven lung cancer.

2.2 Introduction

In cancer cells, dysregulated cell signaling and proliferation occurs through overexpression, post-translational modification or mutation of signaling proteins. RAS is a membrane associated small G protein, which functions as a signaling mediator of receptor and non-receptor tyrosine kinases to cytoplasmic and nuclear effector pathways. Oncogenic mutations of *RAS* account for approximately 30% of all cancers. These mutations results in constitutive signaling, which leads to dysregulated cell proliferation and enhanced survival. Mutations in the *KRAS* gene are common in non-small-cell lung cancer (NSCLC), colorectal, and pancreatic cancer. Approximately 32.2% of patients with lung adenocarcinoma exhibit tumor associated *KRAS* mutations [1]. Uncontrolled cell proliferation as a result of mutations within *RAS* is attributed to a cascade of signaling kinases known as the mitogen activated protein kinase pathway (MAPK). The MAPK pathway includes RAF, mitogen and extracellular signal-regulated kinase (MEK), and extracellular signal-regulated kinase (ERK). The MAPK pathway promotes, by phosphorylation, the activities of several transcription factors, including C-Myc, CREB and C-Fos. This activation leads to the altered transcription of genes that are involved in cell cycle progression. Beyond this, the molecular details of a link between the MAPK cascade and the cell cycle machinery remain partially understood. For example, the molecular basis for the role of MEK and ERK, key components of MAPK signaling in M-phase progression is commonly observed, yet the precise molecular mechanisms have not been defined [2].

Increased abundance of FADD, (mRNA and protein) and specifically the post-translationally modified, phosphorylated and nuclear localized form of FADD is correlated with aggressive disease and poor clinical outcome in lung adenocarcinoma as well as head and neck cancer [3-8]. In addition, amplification of the *FADD* locus on chromosome 11q13.3 is frequently observed in human cancers resulting in increased FADD abundance, poor prognosis [4-7] and correlation with overabundant *CCND1* and *CCNB1*, genes that are involved in the regulation of cell cycle progression [3, 9]. *FADD*-null cells exhibit defects in cell cycle progression [3, 10]. An absence of *Fadd*, as well as expression of a dominant negative *Fadd* mutant in peripheral T lymphocytes, resulted in an inhibition of mitogen-induced T cell proliferation [10-12]. Ten percent of

freshly isolated peripheral T cells from *Fadd*-null mice were arrested in the S and the G2/M phases, compared to two percent from normal littermates **[10]**. Alappat *et al.*, 2005 demonstrated phosphorylation of FADD at Ser194 (Ser191 in mouse), during the G2/M phase, but not in G1/S. Casein Kinase 1 alpha (CK1α) was identified as the kinase responsible for phosphorylation of FADD at Ser194. Alappat *et al.*, 2005 also demonstrated a direct interaction between CK1α and FADD early in mitosis **[13]**. Although a requirement for CK1α dependent phosphorylation of FADD early in mitosis is clear, upstream signaling events and its significance in oncogenesis remain to be investigated. To this end, using conditional mouse models, we demonstrate that mutant *Kras*-mediated lung oncogenesis requires FADD and its phosphorylation by CK1α. Mice in which mutant *Kras* was initiated developed lung tumors as expected, while mice with concurrent introduction of mutant *Kras* and deletion of *Fadd* or *Csnk1a1* exhibited greatly reduced and delayed tumor growth. Embryonic fibroblasts isolated from these animals revealed that activation of *Kras* resulted in the phosphorylation of FADD and enhanced cell proliferation through the MAPK cascade. Phosphorylation of FADD during G2/M and subsequent interaction with key mediators of the G2/M transition, including Polo-Like Kinase 1 (PLK1), Aurora Kinase A (AURKA) and Budding Uninhibited by Benzimidazoles 1 (BUB1), provide a molecular basis for the phenotypes observed in the mouse models.

2.3 Results

2.3.1 A Requirement for FADD in *Kras*-Driven Lung Cancer

A transgenic mouse wherein the genomic locus for *Fadd* is insertionally inactivated and complimented by a conditional transgene (*Fadd:GFP*) **[14]** was crossed with $Kras^{LSL-G12D}$ animals **[15]** and subsequently crossed with $Rosa26^{LSL-Luciferase}$ mice **[16]**. The resulting mouse will be referred to as KF_{Luc} ($Kras^{LSL-G12D}$; *Luc*; *Fadd-/-*). Intranasal instillation of an adenovirus for expression of the Cre-recombinase (AdCre) enabled simultaneous activation of oncogenic *Kras* to initiate tumorigenesis, expression of luciferase as a surrogate for proliferation, and deletion of the *Fadd* transgene (**Fig. 2.1A**). Mice heterozygous for genomic *Fadd* were used as controls since they retained *Fadd* expression despite deletion of the transgene in the lung ($Kras^{LSL-G12D}$; *Luc*;

Fadd+/-) and will be referred to as K_{Luc}. As controls, mice expressing *Fadd* and wild-type *Kras* (*Luc; Fadd+/-*) were also used and will be referred to as *Luc*.

Upon AdCre delivery bioluminescence imaging was performed to monitor tumor growth at indicated time points (**Fig. 2.1, A to C**). A time dependent increase in bioluminescence activity in K_{Luc} was observed at week 7 compared to *Luc* mice (**Fig. 2.1C**). In *KF*$_{Luc}$ animals, we observed minimal changes in bioluminescence activity over time, in contrast to K_{Luc} animals (**Fig. 2.1, B to C**). Animals which were wild type for *Kras* but null for *Fadd (Luc; Fadd-/-)*, hereafter referred to as F_{Luc}, similarly lacked changes in bioluminescence (**Fig. 2.1C**). Anatomic visualization of tumor burden in mice was also carried out using micro-computed tomography (μCT). μCT detectable lesions were identified in K_{Luc} animals, but to a lesser degree in their *KF*$_{Luc}$ littermates, while no detectable lung lesions were identified in mice with wild-type *Kras* (**Fig. 2.1D**). Quantitative analysis of μCT images was accomplished by segmentation and measurement of the functional lung space, which upon subtraction from the total chest space yielded volumetric measure of the tumor and vascular component **[17]**. These analyses, in agreement with the bioluminescence measurements, revealed an increase in the tumor burden at week 13 and 16 in K_{Luc} mice compared to *KF*$_{Luc}$ mice (**Fig. 2.1E**). Using a multimodality reader that allows for simultaneous acquisition of spatially aligned bioluminescence and μCT, demonstrated that the X-ray dense lesions were also positive for bioluminescence. Histological analysis of the single lesion pathologically confirmed a hyper-proliferative phenotype (**Fig. 2.1F**). In agreement with these measurements of tumor burden, we observed prolonged survival in *KF*$_{Luc}$ mice compared to K_{Luc} littermates. The median survival of *KF*$_{Luc}$ mice was 51.4 weeks (95% CI =29.8 to 73.0 weeks) compared to 34 weeks (95% confidence interval of 24 to 44 weeks) for the K_{Luc} mice (**Fig. 2.1G**).

2.3.2 *Fadd*-Null Lung Tumors are Less Proliferative

To confirm our imaging results, we performed histological studies of lung tissue from the aforementioned animals. Histopathological analysis of *KF*$_{Luc}$ and K_{Luc} lungs at 18 weeks post AdCre revealed that K_{Luc} animals often exhibited large adenomas (papillary, solid and mixed), presented large mixed type adenomas (solid and papillary) within lung parenchyma, and possessed alveoli containing atypical adenomatous

38

hyperplasia. A more robust, macrophage predominant, chronic inflammatory infiltrate was also appreciated in these histopathology sections. In contrast, analysis of lung sections from KF_{Luc} animals revealed demonstrably smaller and fewer adenomas. We observed average tumor volumes of 45 uM^2 in the KF_{Luc} mice compared to 70 uM^2 in the K_{Luc} mice (**Fig. 2.2, A to B**). Lung tissue from control *Luc or F$_{Luc}$* animals appeared normal with no detectable hyperplasia.

As a measure of proliferation, Ki-67 immunohistochemistry of lung tissue was also conducted. K_{Luc} tumors demonstrated significantly higher Ki-67 staining, quantitative analysis of 10 animals and 4 fields per animal revealed that almost 30% of cells within K_{Luc} derived tumors were positive for Ki-67, while only 18% of the cells within KF_{Luc} tumors were Ki-67 positive (**Fig. 2.2C**). Consistent with this, lung tissue from KF_{Luc} animals revealed less Cyclin D1 staining compared to K_{Luc} derived tissue by immunohistochemistry as well as western blotting (**Fig. 2.2, A and D**). Tumor samples derived from KF_{Luc} animals also demonstrated lower pRB amounts by western blot, suggesting abrogated cell proliferation (**Fig. 2.2D**). Elevated FADD staining was observed in K_{Luc} derived lung tissue compared to tissue derived from *Luc* or KF_{Luc} animals. Immunohistochemistry of lung sections revealed a low amount of FADD in *Luc* (control) as well as KF_{Luc} animals, while elevated FADD protein was observed in K_{Luc} tumor tissue (**Fig. 2.2A**). High magnification (100x) revealed staining for FADD that was predominantly nuclear in K_{Luc} animals (**Fig. 2.2A**). Western blot analysis of tumor tissue also confirmed a lack of endogenous *Fadd* expression in tumor tissue derived from KF_{Luc} animals compared to K_{Luc} animals. Increased FADD phosphorylation (based on the presence of a doublet of FADD immune-reactive protein at 28kDa **[3, 18-21]**, was consistently observed in tissues wherein mutant *Kras* was activated (K_{Luc}), while a single band was observed in lung tissue from control animals (*Luc*, **Fig. 2.2D**). In addition to Cyclin D1 and pRB, another marker of proliferation, Cyclin B1, was significantly increased in K_{Luc} tumors, but was reduced in KF_{Luc} tumors (**Fig. 2.2D**)*.* A loss of *Fadd* expression resulted in a decrease of pERK1/2 abundance, a downstream mediator of oncogenic KRAS signaling (**Fig. 2.2D** and **Fig. 2.3A**). Since FADD is an established adaptor of Caspase-dependent apoptosis, we also performed immunohistochemical staining for the activated form of Caspase 3 in lung tumor tissue.

Both K_{Luc} and KF_{Luc} lesions lacked staining for active Caspase 3, indicating that differences in tumor size were not due to an increase in apoptotic cell death (**Fig. 2.3B**).

Based on previous experience with conditional mouse models, we hypothesized that tumors arising in KF_{Luc} animals may be FADD positive due to inefficient Cre recombination. To test this, we analyzed the expression of the *Fadd* transgene using semi-quantitative PCR of lung tumors isolated from K_{Luc} and KF_{Luc} mice. Although reduced compared to control tissue, the *Fadd* transgene was still present in all samples tested (**Fig. 2.4A**). Persistent expression the *Fadd* transgene in KF_{Luc} tumors was also observed by western blot and immunohistochemistry (**Fig. 2.2D** and **Fig. 2.4, B to C**).

2.3.3 FADD and FADD Phosphorylation are Required for *Kras*-Driven Cell Proliferation

Since elevated *FADD* mRNA has been shown to correlate with poor survival in lung cancer patients **[3]**, we investigated if *FADD* mRNA amounts correlated with *KRAS* mutation status. Analysis of patient data revealed a correlation between mutant *KRAS* status with increased amounts of *FADD* mRNA as compared to patients with wild type *KRAS* in two independent studies (**Fig. 2.5, A to B**). We next investigated if KRAS signaling impacted phosphorylation of FADD in mouse embryonic fibroblasts (MEF) derived from the mouse models. F_{Luc} derived MEFs lacking mutant *Kras* failed to proliferate in culture due to cell cycle arrest as previously demonstrated **[14]**. Western blot analysis for FADD in *Luc* MEFs revealed a single predominant band at 28kDa, while those from K_{Luc} MEFs exhibited a doublet, indicative of an increase in the phosphorylated form of FADD (**Fig. 2.6A**) **[3, 18-21]**. As expected, KF_{Luc} cells demonstrated no detectable endogenous FADD. Consistent with our finding for a role of FADD in proliferation, we observed increased Cyclin D1 abundance in MEFs from K_{Luc} compared to the KF_{Luc} (**Fig. 2.6A**). K_{Luc} MEFs exhibited a higher rate of proliferation compared to KF_{Luc} and *Luc* MEFs (**Fig. 2.6B**). This finding was in agreement with previous work wherein decreased proliferation was observed in *Fadd-/-* MEFs compared to *Fadd+/-* MEFs **[14, 21, 24]**. Reconstitution of *Fadd* expression in KF_{Luc} cells restored cell proliferation (**Fig. 2.6B**). To evaluate a requirement for CK1α, the kinase responsible for FADD phosphorylation **[12, 25-26]**, K_{Luc} cells were treated with a CK1α inhibitor, CKI-7. In the treated K_{Luc} cells, we observed a marked decrease in

proliferative ability whereas proliferation of KF_{Luc} or *Luc* cells was not significantly impacted by the inhibitor (**Fig. 2.6C**). Since increased abundance of phosphorylated FADD were observed in K_{Luc} cells compared to then *Luc* cells, we hypothesized that MEK and ERK, key effectors of the RAS signaling pathway, may be upstream mediators of FADD phosphorylation. Lonafarnib, an inhibitor of *Kras* farnesylation **[27]**, as well as PD0325901, a MEK inhibitor **[28]** inhibited proliferation and FADD phosphorylation (**Fig. 2.6, C and F**). In soft agar colony formation assays, KF_{Luc} MEFs formed 70% fewer colonies as compared to K_{Luc} MEFs (**Fig. 2.6D**). Exogenous *Fadd* expression in KF_{Luc} cells restored colony forming capacity, confirming a requirement for FADD in proliferation (**Fig. 2.6D**). K_{Luc} cells treated with CKI-7, PD0325901 or Lonafarnib also reduced colony forming activity as compared to untreated cells (**Fig. 2.6D**).

Examination of the cell cycle distribution revealed that compared to K_{Luc} cells, KF_{Luc} cells were arrested in G2/M **(Fig. 2.6E)**, and reconstitution of *Fadd* restored normal cell cycle distribution (**Fig. 2.6E**). Cell cycle analysis of CKI-7 treated K_{Luc} cells revealed a G2/M arrest analogous to untreated *Fadd*-deficient KF_{Luc} cells, whereas PD0325901 or Lonafarnib treatment resulted in a G1 arrest (**Fig. 2.6E**). CKI-7 treated K_{Luc} cells showed a marked decrease in pRB and Cyclin D1 and an increase in phosphorylated Cell Division Cycle 2 (pCDC2), confirming an arrest of cells at G2/M (**Fig. 2.6F**). The amount of phosphorylated FADD was also decreased upon treatment with CKI-7 (**Fig. 2.6F**). Treatment with Lonafarnib or PD0325901 also resulted in decreased amount of pRB and Cyclin D1 as well as phosphorylated FADD (**Fig. 2.6F**).

2.3.4 FADD Interacts with Key Mediators of G2/M Transition.

To study the phosphorylation of FADD as cells transit G2/M, H1975 human lung cancer cells were synchronized by a double thymidine block. FADD-phosphorylation was prominent eight hours post-release, which coincided with a peak in Cyclin B1 and AURKA amounts, but was preceded by a an increase in PLK1 abundance (**Fig. 2.7A**), events which mark the transition of cells from G2 into M **[29-30]**.

We next conducted an interactome study using Halo-tagged FADD in HEK 293T cells. Mass spectrometry analysis of co-precipitating polypeptides revealed the interaction of FADD with CK1α as well as several proteins involved in the cell cycle, including PLK1, CDC20 and Aurora Kinase B (AURKB*)* (**Fig. 2.7B**). To evaluate if

interaction of FADD with these proteins was specific for G2/M, A549 lung cancer cells were treated with hydroxyurea to induce a G1/S arrest, or with nocodozole to induce a G2/M arrest (**Fig. 2.7C**). Immunoprecipitation analysis revealed an interaction of FADD with PLK1 predominantly in G2/M. Since PLK1, AURKB and CDC20 interact with BUB1 during G2/M **[33-35]** we investigated if BUB1 also interacted with FADD. Indeed, BUB1 and AURKA maximally interacted with FADD in G2/M compared to G1/S arrested or asynchronous cells. Inhibition of CK1α using CKI-7 abrogated the interaction of FADD with AURKA, PLK1 and BUB1 (**Fig. 2.7C**). Functional annotation analysis of the interactome using DAVID (**Fig. 2.8, A to B**) **[31-32]** also identified other FADD-interacting nodes, including proteins involved in cell death, a pathway in which FADD was originally studied in **[18]**.

2.3.5 A Requirement for CK1α in *Kras*-Driven Lung Cancer

To investigate a requirement for CK1α in *Kras*-driven lung oncogenesis a mouse model was generated wherein the genomic locus of *Csnk1a1* could be conditionally deleted (*Csnk1a$^{fl/fl}$*) **[36]** in the presence of mutant *Kras* expression. *Kras$^{LSL-G12D}$*; *Rosa26$^{LSL-Luciferase}$* animals **[15, 16]** were crossed with *Csnk1a$^{fl/fl}$* to generate *KC$_{Luc}$* mice (*Kras$^{LSL-G12D}$*; *Luc*; *Csnk1a$^{fl/fl}$*). Intranasal instillation of an adenovirus for expression of AdCre was performed to initiate *Kras*-mediated tumorigenesis in the presence (*K$_{Luc}$*) or absence of *Csnk1a1* expression (*KC$_{Luc}$*, **Fig. 2.9A**). Littermates with wild-type *Kras* in the presence (*Luc*) or absence of *Csnk1a1* (C$_{Luc}$) were used as controls (**Fig. 2.9A**). Imaging revealed a robust increase in bioluminescence, indicative of tumor burden, in *K$_{Luc}$* mice compared to the *Luc* mice (**Fig. 2.9B**) as seen previously (**Fig. 2.1, B and C**). In contrast, *KC$_{Luc}$* and *C$_{Luc}$* mice did not show an increase in bioluminescence over time, indicative of decreased tumorigenesis. µCT confirmed the presence of lung tumor burden in *K$_{Luc}$*, whereas no detectable tumors were observed in *KC$_{Luc}$*, *C$_{Luc}$* and *Luc* mice (**Fig. 2.9C**). Quantitative analysis of µCT images was performed, which revealed a 6 fold decrease in tumor burden at week 18 in *KC$_{Luc}$* mice compared to *K$_{Luc}$* (**Fig. 2.9D**).

Histological analysis of lung sections from the *KC$_{Luc}$* mice at week 18 demonstrated minimal hyperplasia and a rare adenoma compared to *K$_{Luc}$* mice (**Fig. 2.9E** and **Fig. 2.10**). Lesions present in *KC$_{Luc}$* mice stained positive for CK1α, indicating that they arose from cells where only *Kras* was activated, but *Csnk1a1* was not Cre-

recombined (**Fig. 2.10**). Both *Luc* and C_{Luc} mice showed healthy lung tissue as expected. K_{Luc} lung tumors showed increased quantities of FADD, which was also nuclear localized, whereas in KC_{Luc}, C_{Luc} and *Luc* mice, lower amounts of FADD were observed (**Fig. 2.9E**).

To investigate if ablation of *Csnk1a1* expression resulted in a decrease in FADD-phosphorylation, we isolated MEFs from KC_{Luc} animals and treated with increasing titers of AdCre. A decrease in FADD-phosphorylation was observed when in the absence of *Csnk1a1* expression (**Fig 2.9F**). Since CK1α is also known to play a role in p53 signaling through phosphorylation of Mouse Double Minute 2 (MDM2) and Mouse Double Minute X (MDMX), as well as in Wnt signaling through by phosphorylation of β-Catenin **[37-39]**, we next asked if ablation of *Csnk1a1* in our KC_{Luc} MEFs stimulates these signaling pathways. The abundance of p53 and the amount of phosphorylated MDM2 were unchanged in KC_{Luc} compared to K_{Luc} animals (**Fig 2.9G**). Similarly, the amount of β-Catenin was unchanged although phosphorylated β-Catenin (Ser45) levels were lower (**Fig 2.9G**).

2.4 Discussion

The constitutive activation of KRAS, through dysregulated EGFR signaling or mutations in *KRAS*, leads to enhanced proliferation through the RAS-MEK-ERK axis. Mutations in the small GTPase *KRAS* renders the protein constitutively active by locking GTP in its binding pocket **[40]**. The G12D mutation of *KRAS* is present in 17% of patients with lung cancer **[41]**. Mutually exclusive to this, genomic amplification and/or overexpression of EGFR are also commonly found in patients with lung cancer **[1]**. Erlotinib and Gefitinib, small molecule kinase inhibitors targeting the EGFR, have shown significant efficacy but in a limited set of patients. In addition, development of drug resistance due to mutations of *EGFR* and compensatory signaling through alternate receptor tyrosine kinases has limited the broad applicability of these therapies. Recent progress in targeting $KRAS^{G12C}$ is encouraging **[42]**, but KRAS inhibitors are currently not clinically available. Efforts to target downstream effectors of KRAS, including MEK, are in development however, preliminary evidence indicates that these may not be effective as monotherapies **[43]** due to compensatory signaling through the PI3K/AKT pathway. The EGFR-KRAS-MEK-ERK signaling axis represents

a major mitogenic pathway in cancer, yet the molecular details of signaling events downstream of RAS and MEK that lead to cell cycle proliferation are not well understood. This may explain the paucity of molecular targets for abrogating EGFR and KRAS mitogenic signaling.

The studies presented here demonstrate that phosphorylation of FADD by CK1α represents a key signaling event in *KRAS*-mediated mitogenic signaling. Genetically engineered conditional mouse models were used to initiate lung cancer in the presence or absence of *Fadd* or *Csnk1a1*. Ablation of either resulted in a decrease in the oncogenic potential of mutant *Kras*. Tumor progression was delayed significantly in the absence of *Fadd* or *Csnk1a1* as revealed by bioluminescence and μCT imaging. In support, histopathological studies revealed fewer and smaller lesions in KF_{Luc} as well as KC_{Luc} mice compared to K_{Luc} animals. Expression of mutant *Kras* resulted in an increase in FADD protein, as well as its phosphorylated form in tumor tissue as well as MEFs derived from these animals. Inhibition of KRAS, MEK or CK1α resulted in a reduction of FADD phosphorylation. Decreased FADD phosphorylation in response to MEK inhibition has been described previously **[44]**, further affirming our finding that phosphorylation of FADD represents an important signaling event downstream of the KRAS-MEK-MAPK pathway**.**

Immunohistochemical analysis of tissue from K_{Luc} revealed increased abundance of markers of cell proliferation including Ki-67 and Cyclin D1. In support, tumors isolated from these animals exhibited elevation in markers of proliferation including Cyclin D1, pERK1/2, pRB, Cyclin B1. In contrast, loss of *Fadd* or *Csnk1a1* did not show an increase in these markers of cell proliferation in tissues and MEFs derived from KF_{Luc} or KC_{Luc} mice, suggesting a requirement for FADD and its phosphorylation by CK1α in mutant *Kras*-mediated mitogenic signaling. This was further supported by an observed G2/M arrest of MEFs lacking *Fadd*, or wherein its phosphorylation was inhibited. Previous findings demonstrate a role for FADD, specifically its phosphorylated form, in the proliferation of T cells **[10, 12, 14, 20]**. This complements our findings that FADD and its phosphorylation are required for *Kras*-mediated cell proliferation. Additionally, in *FADD*-null Jurkat cells which arrest in G2/M, reconstitution of either a *FADD* phospho-mimetic (FADD-Asp) or a non-phosphorylatable form (FADD-Ala) failed to complement

44

the *FADD*-null phenotype [3]. The AK2/DUSP26 phosphatase protein complex has been shown to result in the dephosphorylation of FADD [21]. Reduced amounts AK2 in tumor cells and human cancer tissues correlated with elevated amounts of phosphorylated *FADD* and proliferation. Consistently, $AK2^{+/-}$ MEFs as well as AK2 knockdown exhibited an increase in phosphorylated FADD abundance and enhanced cell proliferation, which could be reversed by ectopic AK2 expression, further supporting a role for phosphorylated FADD in mitogenic signaling.

Controlled phosphorylation/dephosphorylation reactions of complexes such as the cyclin B/cyclin-dependent kinase 1 (CDK1) are central to the control of mitosis [45]. Phosphorylation of FADD in a cell cycle dependent manner [3, 13] (**Fig. 2.6 F** and **Fig. 2.7A**), the G2/M arrest of cells lacking FADD [3] (**Fig. 2.6E**), and the G2/M arrest of cells wherein FADD-phosphorylation is inhibited (**Fig. 2.6E**) are all consistent with a role for FADD-phosphorylation in cell cycle progression in response to *Kras* activation. Maximal phosphorylation of FADD prior to histone H3 (Ser10) phosphorylation [*46*] and the interaction of FADD with PLK1, AURKA, CDC20 and BUB1, all mediators of the G2/M transition, further support its role in G2/M transition. The interaction of FADD with PLK1 and AURKA has been demonstrated previously [29], but our findings show that these occur in a G2/M specific manner and in the context of mitogenic signaling by mutant *KRAS*.

Previous studies describing the conditional deletion of *Csnk1a1* in the intestine resulted in activation of the Wnt pathway. Concurrent deletion of p53 resulted in activation of the Wnt pathway and resulted in invasive carcinomas [36]. Our analysis of MEFs derived from KC_{Luc} or C_{Luc} animals did not reveal dysregulated Wnt signaling. This discrepancy could be explained by the cellular context (intestinal tissue compared to lung tissue or MEFs) as the Wnt pathway has been primarily associated with colon cancer and lung metastasis [22, 47].

In summary, using a murine model of lung cancer we demonstrate a requirement for FADD in *Kras*-mediated tumorigenesis, and demonstrate that phosphorylation of FADD by CK1α is required for mitogenic activity of the KRAS-MEK-ERK signaling pathway. Upon phosphorylation, FADD is translocated to the nucleus [3-4, 14, 20, 24] wherein it is required for G2/M progression through its interaction with PLK1, AURKA,

CDC20 and BUB1 (**Fig. 2.11**). Our finding of increased in *FADD* mRNA expression in patients with mutant *KRAS* emphasizes the significance of the signaling pathway in *KRAS*-mediated oncogenesis. We propose that CK1α may be an attractive downstream target for inhibition of oncogenic signaling in EGFR and mutant *KRAS*-driven tumors.

2.5 Materials and Methods

Mice

All animal protocols were approved by the University of Michigan University Committee on Use and Care of Animals (UCUCA). All mouse work was performed in accordance with the University of Michigan protocol P00004781. Animals were housed in specific pathogen-free facilities of the University of Michigan Biomedical Science Research Building. *Kras$^{LSL-G12D}$* mice [15] from the NCI repository were intercrossed with *Rosa26$^{LSL-Luciferase}$* (Jackson Laboratory, stock# 005125) and *Fadd-/-; Fadd:GFP* [14] (provided by Jianke Zhang, Thomas Jefferson University) mice to create *Kras^{G12D}*; *Luc*; *Fadd-/-* or *Fadd+/-* animals (*KF$_{Luc}$* or *K$_{Luc}$*, respectively). Combinations of mutant littermates were used as controls: *Luc*; *Fadd+/-* or *Luc*; *Fadd-/-* (*Luc* or *F$_{Luc}$*). A Kaplan-Meier survival curve was performed to represent animals that needed to be euthanized, if signs of labored breathing were present, or died during the time of experiments. *Csnk1a$^{fl/fl}$* mice [36] (provided by Yinon Ben-Neriah and Eli Pikarsky) were also crossed with *Kras$^{LSL-G12D}$* mice and *Rosa26$^{LSL-Luciferase}$* mice to create *Kras$^{LSL-G12D}$; Luc; Csnk1a1$^{fl/fl}$* or *Csnk1a1+/+* animals (*KC$_{Luc}$* or *K$_{Luc}$* respectively) and combinations of littermates were used as controls *Luc; Csnk1a +/+* or *Luc; Csnk1a$^{fl/fl}$* (*Luc* or *C$_{Luc}$*).

Genotyping and PCR

Mice were genotyped using tail DNA. For the genotyping of mutant *Kras$^{LSL-G12D}$*, wild type *Kras* and Cre-recombined *Kras$^{LSL-G12D}$*, three primers were used: 5'GTCTTTCCCCAGCACAGTGC, 5'CTCTTGCCTACGCCACCAGCT and 5'AGCTAGCCACCATGGCTTGAGTAAGTCTGCA. For *Rosa26$^{LSL-Luciferase}$* the primers used were 5' CGTGATCTGCAACTCCAGTC and 5'GGAGCGGGAGAAATGGATATG. For the *Fadd* wild type allele the following primers were used: 5' TGCGCCGACACGATCTACTG and 5' TGTCAGGGTGTTTCTGAGGA. For the *Fadd* knockout neo cassette the primers were: 5' CGCTCGGTGTTCGAGGCCACACGC and 5' ACTGTAGTGCCCAGCAGAGACCAGC. For the *Fadd* transgene (*Fadd:GFP)*, the primers were 5' GTTGTCTTCGAAGTGCTCAGGC and 5' GAACTTGTGGCCGTTTACGTC. For the genotyping of wild type and *Csnk1a1$^{fl/fl}$* mice the following primers were used 5' TCCACAGTTAACCGTAATCGT and 5'

AACTGCAAATGAAAGCCCTG The *Fadd:GFP* primers were utilized for semi-quantitative PCR to determine Cre recombination efficiency. 10ng of template were used and the PCR was run for 25 cycles.

Induction of lung cancer

Lung tumors were initiated with 3×10^7 plaque forming units of Adenovirus-Cre Recombinase, by intranasal inhalation in mice 6 to 8 weeks in age **[48]**.

Mouse Bioluminescent Imaging

Mice were imaged at weeks 7, 13, 18 and 22 post Adenovirus-Cre Recombinase administration. Imaging was performed on an IVIS Spectrum from Perkin Elmer. Mice were injected with 150mg/kg D-Luciferin (Promega)/PBS solution and anesthetized with 1-2% isoflurane/air while imaged. Serial images were acquired for 30 seconds to 2 minutes intervals for 20 minutes post injection to capture the peak luminescence. Regions of interest were drawn around each lung and a highest photon emission value for each image was used for analysis.

Micro-computed Tomography

μCT imaging was performed at weeks 13 and 16 or 18 post adenovirus Cre recombinase administration using a Siemens Inveon System with the following parameters: 80kVp, 500μA, 400-ms exposure, 360 projections over 360 degrees, and 49.2-mM field of view (56-μM voxel size). Quantitative analysis was performed on automatically segmented lung volumes as the sum of lung, tumor, and vascular tissues. Following image calibration to Hounsfield units (HU) using air and a water phantom, segmentation of the lungs was accomplished using a connected threshold algorithm developed in-house (Matlab, Natick, MA) with a threshold of -200HU. This volume was subtracted from the total chest volume to approximate the tumor plus vascular volume. An assumption with this analysis is that vasculature should be similar between all subjects, with changes in this volume indicative of tumor volume changes **[17]**.

BLI/CT Imaging

CT and BLI imaging was performed to demonstrate co-localization of luminescence with CT-determined lung lesions at 22 weeks post adenovirus Cre recombinase administration using an IVIS Spectrum CT from Perkin-Elmer. Mice were injected with 150mg/kg D-Luciferin (Promega)/PBS solution and anesthetized with 1-2% isoflurane/air while imaged at 1 minute intervals. The following parameters for CT imaging were used: 50kVp, 1mA, 720 projections over 360 degrees, and 12-cm field of view (150µm voxel size).

Histology

Animals were euthanized and the lung was perfused with PBS through the heart. The lung was removed and fixed in formalin for 24 hours. Samples were embedded in paraffin and sliced at 5µM. Samples were stained with hematoxylin and eosin y (H&E). Protocol in brief: Samples were hydrated in xylene, 100% EtOH, 95% EtOH and water. Samples were then stained in Gill Hematoxylin washed in tap water. Samples were immersed in 95% EtOH and then stained with acidic eosin y. All antibodies were used at 1:200 and secondary antibodies used were biotinylated-rabbit or biotinylated-goat using the DAP system and Alexa488-chicken for immunofluorescence.

Antibodies and Reagents

Rabbit polyclonal antibodies to GFP, pERK1/2, pRB, ERK1/2, Cyclin D1, phospho-FADDS194, AURKA, phospho-β-Catenin, β-Catenin, pMDM2 and PLK1 were purchased from Cell Signaling Technology (Danvers, MA). The antibody for human FADD was obtained from BD Biosciences (San Jose, CA). Antibodies against Cyclin B1, CK1α, MDM2 and p53 were purchased from Santa Cruz (Santa Cruz, CA). The antibody against mouse FADD used for western blotting was purchased from Epitomics, initially (Burlingame, CA (cat# 3523-1)), and then from Abcam (Cambridge, MA (cat# ab124812)). Antibodies for BUB1, β-Actin, FADD (mouse FADD) and GFP (used for IHC and IF, respectively) antibodies were from Abcam (Cambridge, MA (FADD cat# ab24533). Ki-67 antibody was obtained from Vector labs. CKI-7 was from Sigma (St. Louis, MO). PD0325901 was purchased from Selleck (Houston, TX), and Lonafarnib

was bought from Cayman Chemical (Ann Arbor, MI). Alamar Blue was purchased from Invitrogen (Carlsbad, CA). Luciferin was obtained from Promega (Madison, WI). Adenovirus-Cre was bought from the University of Michigan Vector core.

Tissue Isolation and Western blotting

Animals were euthanized with CO_2. Tumors were harvested and snap frozen in liquid nitrogen. Tumor samples were manually homogenized in RIPA buffer (Invitrogen) with protease inhibitor (Complete-Roche), PhosSTOP (Roche), and PMSF (Sigma). Lysates were centrifuged at 4^oC for 30 minutes at 16,000xg and the supernatant collected for analysis. Cells from culture dishes were collected in cold 1x PBS and centrifuged at 1,800 X g for 5 minutes at 4°C. The cell pellet was washed with cold PBS and then lysed with the same buffer as above. Cells in lysis buffer were incubated in ice for 30 minutes. The lysates were then cleared by centrifugation at 16,000 X g for 15 minutes. The collected supernatants were estimated for protein content by Lowry assay (Biorad). Lysates with equal amounts of protein were resolved by 12% SDS/PAGE, and protein abundance was detected by Western blot analysis using the appropriate primary and secondary antibodies. Specific signals were visualized by using ECL Clarity western detection system by Biorad.

Cell Culture, MEF Isolation

A549 (lung epithelial carcinoma), NCI H1975 (lung epithelial adenocarcinoma) and HEK293T cells were purchased from the American Type Culture Collection (ATCC). A549 and H1975 cell lines were cultured in RPMI-1640 (Invitrogen, Carlsbad, CA) supplemented with 10% fetal bovine serum (FBS) and 1% penicillin, streptomycin and glutamine (Invitrogen, Carlsbad, CA). HEK293T cells were cultured in DMEM (Invitrogen, Carlsbad, CA) and supplemented with 10% FBS and 1% penicillin, streptomycin and glutamine. Mouse embryonic fibroblasts (MEFs) were isolated from day E13-14 embryos from one mother. Briefly embryos were placed in ice cold PBS where the placenta and visceral tissue was removed. After washing in PBS the embryos were minced in trypsin and incubated at 37°C. The minced embryos were then further disrupted and then plated with DMEM supplemented with 10% FBS, and 1% of

penicillin, streptomycin, glutamine and non-essential amino acids (Invitrogen, Carlsbad, CA). Cells were grown at 37°C with 5% CO_2. MEFs were subjected to AdCre 1×10^8 pfu and 24-48 hours later were FACs sorted for GFP negative cells.

Cell Proliferation, Soft Agar Foci Assays, and Cell Cycle Analysis

Cell proliferation assays were carried out by plating 3×10^3 MEF cells per well in a 96 well format in DMEM supplemented with 10% FBS, 1% penicillin streptomycin with glutamine and 1% non-essential amino acids. 5 hours after plating, 250µM CKI-7, 10 µM Lonafarnib or 200nM PD0325901 were added to designated wells. 24 hours after adding CKI-7 Lonafarnib or PD0325901, 10ul of Alamar blue was added to the first set of wells. Fluorescence was measured an hour later on a Perkin Elmer Envision. This was repeated at 48, 72 and 96 hours post addition of inhibitors. For the soft agar assay 2×10^4 MEF cells were plated in 0.3% agarose DMEM complete, with 20% FBS, on top of 0.7% agar supplemented with DMEM. Media was added to the cells twice a week for 2 weeks. 0.005% crystal violet was added to the cells and colonies were counted 24 hours later using a dissecting microscope and ImageJ. For cell cycle analysis, MEF cells were plated in supplemented DMEM as described above. 24 hours later 250µM CKI-7, 10µM Lonafarnib or 200nM PD0325901 were added. 24 hours after adding the inhibitors, cells were trypsinized and resuspended with PBS. Cells were then fixed with 100% ice cold ethanol either for 20 minutes. Cells were centrifuged and resuspended with a propdium Iodide and RNAse solution (final concentration 50µg/ml PI with 100µg/ml RNAse Type I-A in PBS). Cells were incubated at room temperature for 20 minutes and then over night at 4°C in the dark before being analyzed. Cells were analyzed as described above using a FACSAria III machine and with the FlowJo software.

Thymidine Synchronization, Immunoprecipitation

To detect the cell cycle dependent endogenous association between FADD and other cell cycle related proteins, NCI H1975 cells were synchronized by double thymidine block. Cells were incubated with 4 mM thymidine (Sigma) for 16 hours, released into fresh media for 9 hours, followed by 16 hours thymidine incubation then released into

fresh media. Cells were harvested at the indicated time points. Synchronized cells were harvested in lysis buffer (50 mM Tris-HCl pH 7.5, 150 mM NaCl, 10% glycerol, 1 mM EDTA, 1% NP40) supplemented with protease and phosphatase inhibitors. Protein concentration was normalized by Biorad Protein Assay (Bio-Rad). Immunoprecipitation was carried out by incubating cell lysates with antibodies against human FADD or normal mouse IgG for 2 hours at 4°C. Antibody-protein complexes were captured with protein A or G-sepharose (GE Healthcare) by incubating 50 µl of beads per 200 µg of protein at 4°C for 2-3 hours. The resulting pellet was collected by centrifugation at 2,000g for 2 minutes, washed three times with lysis buffer, boiled in 2X NuPage LDS sample buffer (Invitrogen) and resolved by SDS-PAGE. Western blots were carried out as outlined above.

Mass Spectrometry

12 million HEK 293T cells in 15 cm dishes were transfected with 30 µg pFN21A-FADD-HaloTag and Ctrl-HaloTag using Fugene HD. 24 hours post transfection, cells were scraped into DPBS and cell pellets were frozen at -70C for at least 20 minutes. Previously frozen cell pellets were lysed in Promega Mammalian Lysis Buffer supplemented with protease inhibitor cocktail (G65A). The cleared lysate was bound to the pre-equilibrated HaloLink resin for 15 minutes at room temperature. Resin-bound proteins were eluted with Promega SDS Elution Buffer (G651A). Samples were analyzed by LC-MS/MS analysis. Refer to Promega TM342 Section 5A for details.

Statistics

Differences between groups were assessed using an unpaired Student's t-test. Results were declared statistically significant at the two-tailed 5% comparison-wise significance level ($p < 0.05$). All error bars represent the standard error of the mean (SEM).
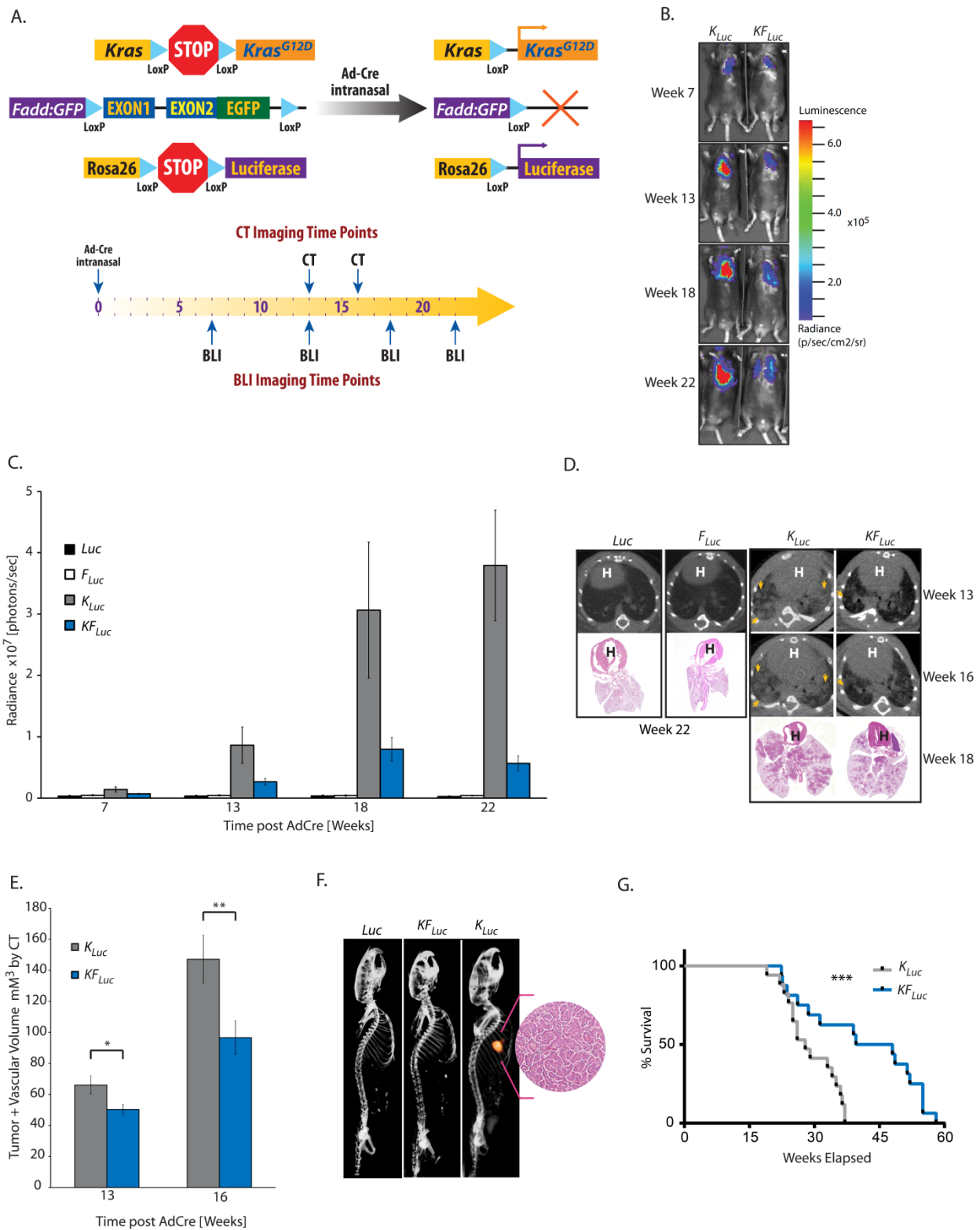
2.6 Figures

Figure 2.1 A requirement for FADD in *Kras*-driven lung cancer
(**A**) Genetic strategy used to activate $Kras^{LSL-G12D}$, $Rosa26^{LSL-Luciferase}$ and deplete *Fadd:GFP* expression in a lung specific manner. Animals were imaged using bioluminescence and/or CT at indicated weeks post administration of AdCre. (**B**) Representative bioluminescent images of K_{Luc}, and KF_{Luc} mice at designated times. (**C**) Average bioluminescence (BLI) for *Luc* (n=7), F_{Luc} (n=7), K_{Luc} (n=25), and KF_{Luc} (n=34) mice at specified times. (**D**) Representative images of CT scans of lungs from *Luc*, F_{Luc}, K_{Luc}, and KF_{Luc} animals at shown times, with H&E slide corresponding to that animal from week 18 or week 22 as indicated. Arrows indicate lesions. H indicates heart. (**E**) Average tumor and vascular volumes of K_{Luc} (n=10) and KF_{Luc} (n=17) analyzed from CT at indicated times. Statistical significance *p=0.009 and **p=0.018 calculated using an unpaired Student's t-test. (**F**) Co-localization of BLI and CT image of *Luc*, KF_{Luc} and K_{Luc} mice. Inset of H&E stained image of lesion in K_{Luc} animal. (**G**) Survival Plot of K_{Luc} (n=19) and KF_{Luc} (n=15). ***p=0.005 determined by Wilcoxon logrank test. All data are represented as the mean $\pm$ SEM.
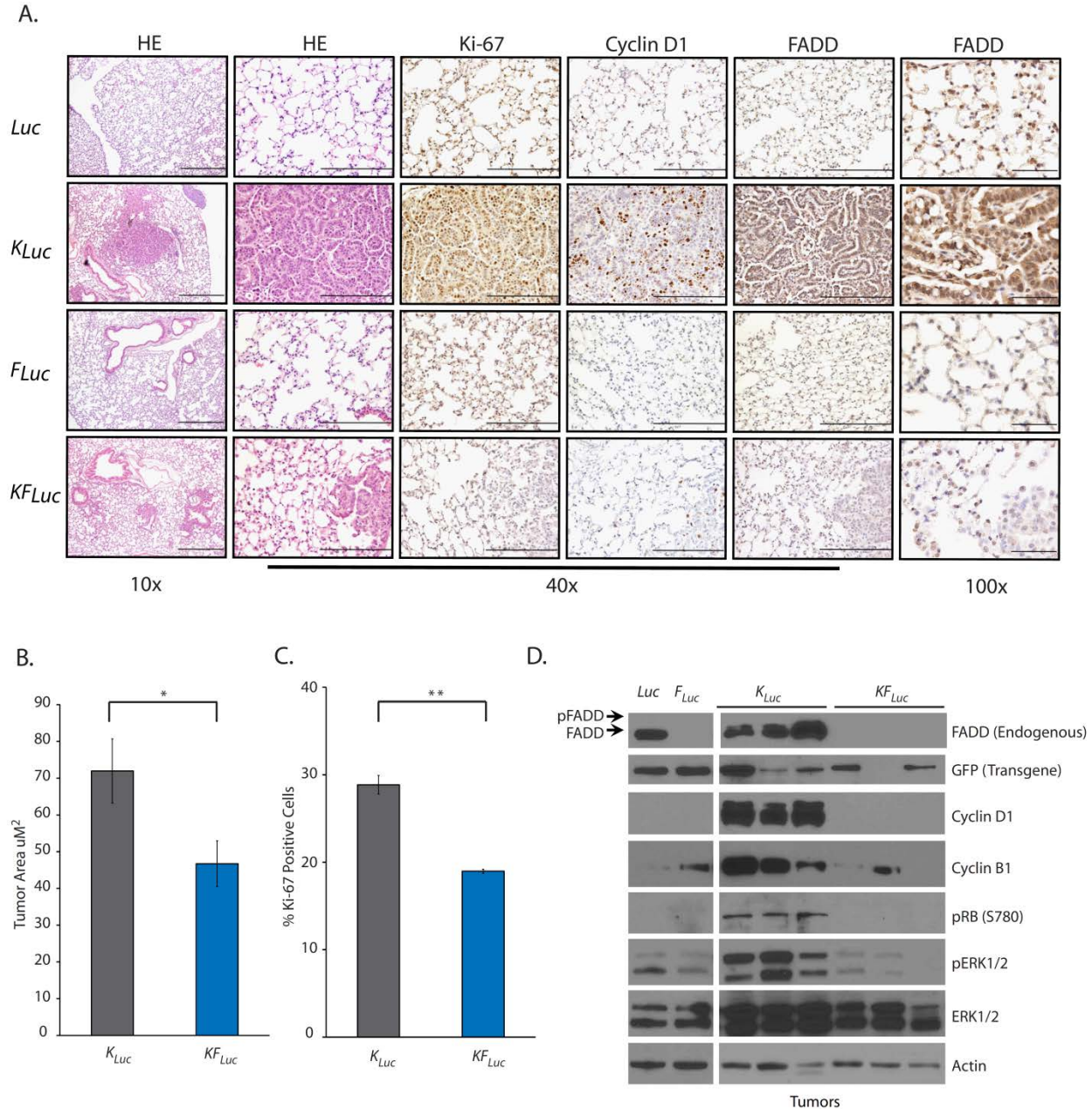
Figure 2.2 *Fadd*-null lung tumors are less proliferative
(**A**) Representative images of lung histology from 18 weeks post AdCre animals stained with hematoxylin and eosin (H&E) and antibodies against Cyclin D1, Ki-67, and FADD. Scale bar = 500uM for 10x, 200uM for 40x, and 50uM for 100x. (**B**) Average tumor area quantified from H&E slides of K_{Luc} (n=6) and KF_{Luc} (n=10) mice. *p=0.04 calculated using unpaired Student's t-test. (**C**) Average percentage of positive Ki-67 stained cells of K_{Luc} (n=10) and KF_{Luc} (n=10) mice. **p=2×10^{-5} calculated using unpaired Student's t-test. (**D**) Representative western blot of lung tumor protein using antibodies for FADD (endogenous), GFP (*Fadd* transgene), pERK1/2, total ERK1/2, phospho-RB, Cyclin D1, Cyclin B1 and β-Actin.
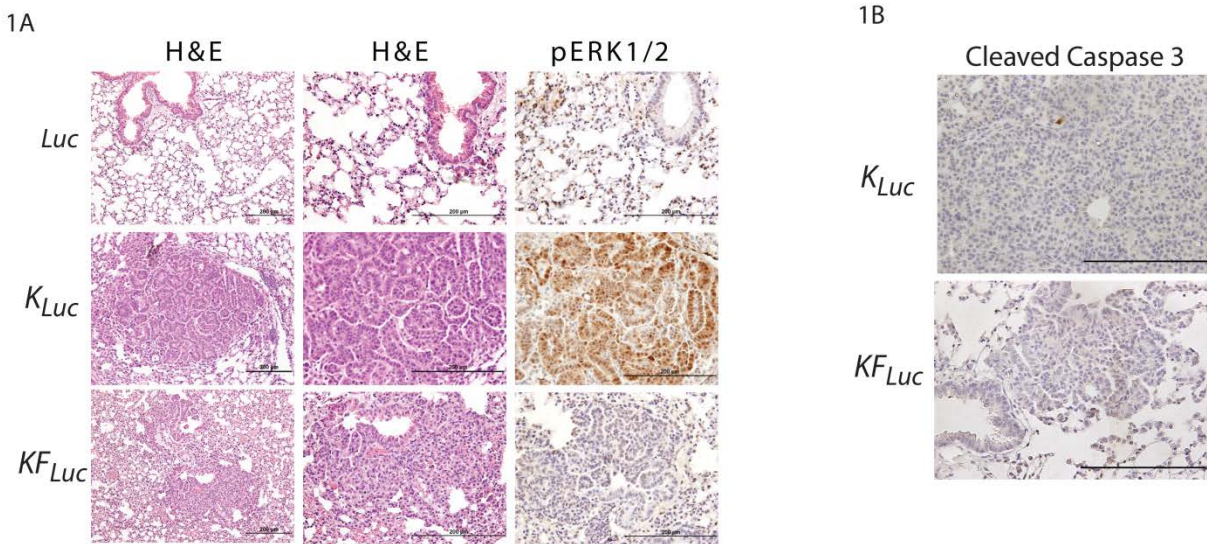
Figure 2.3 *Fadd*-null lesions have lower pERK1/2 abundance and their smaller size is not due to cell death (A) Representative images of lung tissue from *Luc*, *K~Luc~* and *KF~Luc~* stained with an antibody to pERK1/2 or Hematoxylin and Eosin Y (H&E). Scale bar =200uM. (**B**) Representative images of lung tissue from *K~Luc~* and *KF~Luc~* animals stained with an antibody against cleaved-Caspase 3 at 40x magnification. Scale bar = 200uM
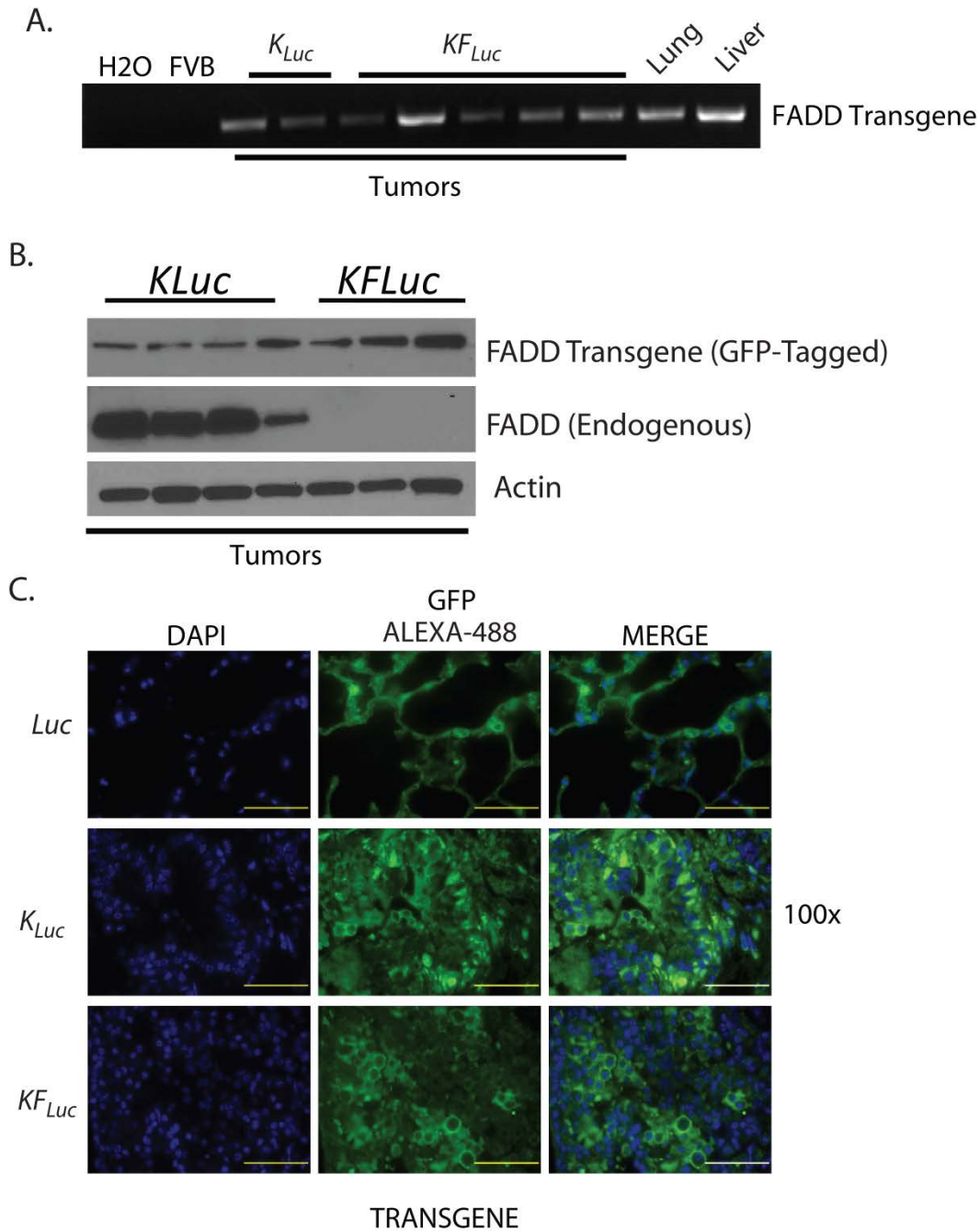
Figure 2.4 *Fadd*-null lesions still express *Fadd* transgene. (A) Semi-quantitative PCR of tumor samples from individual mice show decreased quantities of *Fadd* transgene (*Fadd:GFP*) compared to liver samples. (**B**) Representative western blot of tumor samples from individual K_{Luc} and KF_{Luc} mice probed with antibodies against FADD, GFP and β-actin. All samples are positive for *Fadd* transgene (GFP). (**C**) Immunofluorescence of tumor tissue stained with DAPI and an antibody against GFP. Scale bar = 500uM.
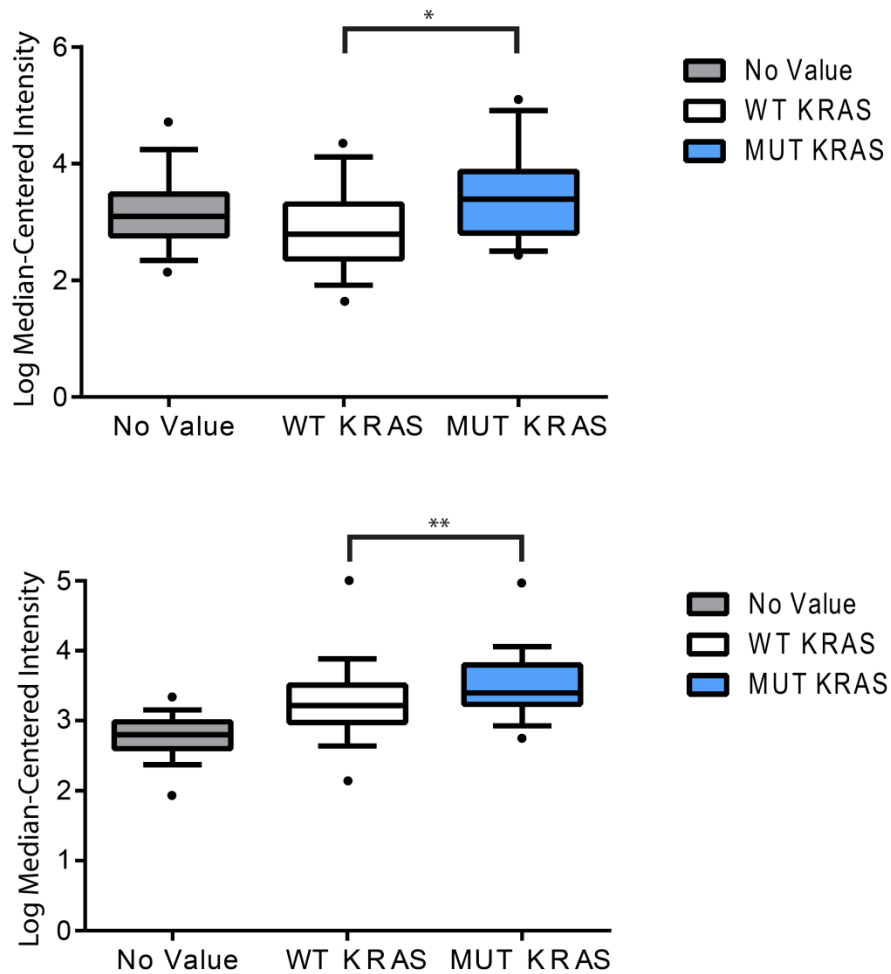
Figure 2.5 Increased *FADD* mRNA correlates with *KRAS* mutation. (**A**). Box and whiskers graph analyzed from Oncomine using data from Ding *et al* 2008 (*22*). Patient data was separated based on mutant *KRAS* status. Patients' whose *KRAS* mutation status was unknown was placed in a No Value (n= 34) group. *FADD* mRNA was increased in patients with mutant *KRAS* (n=12) as compared to patients with wild type *KRAS* (n=29). The P value was calculated using unpaired Student's ttest comparing. p=0.007. (**B**). Box and whiskers graph analyzed from Oncomine using data from Okayama *et al* 2012 (*23*). Patient data was separated based on mutant *KRAS* status. Patients' whose *KRAS* mutation status was unknown was placed in a No Value (n=20) group. *FADD* mRNA was increased in patients with mutant *KRAS* (n=20) as compared to patients with wild type *KRAS* (n=206). The P value was calculated using unpaired Student's ttest comparing. p=0.009.
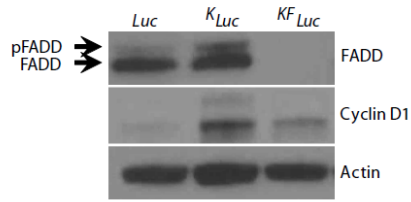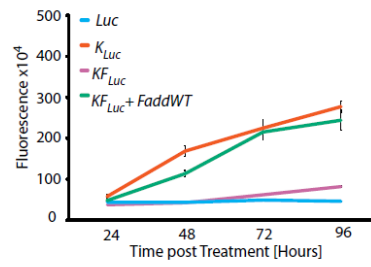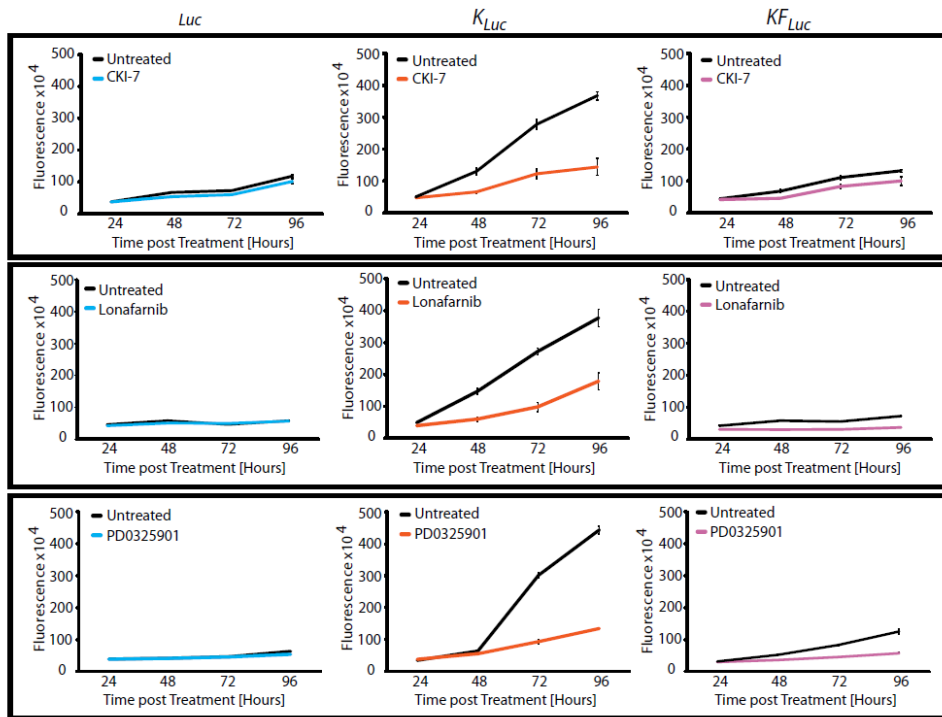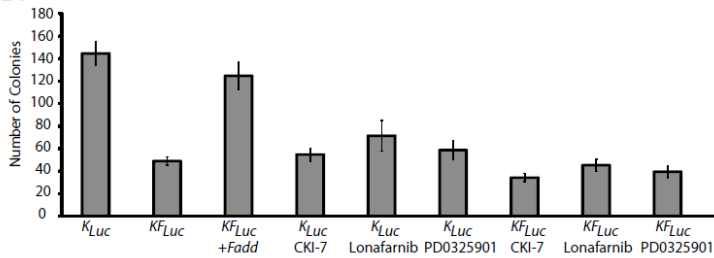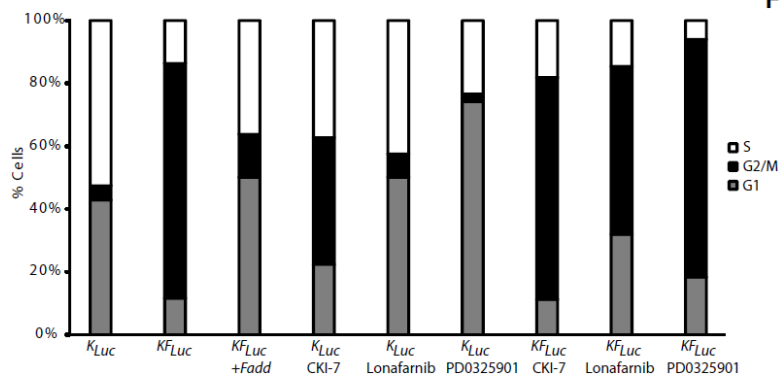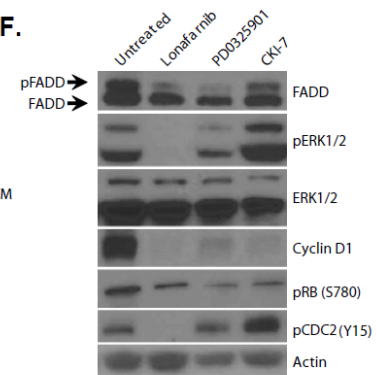
Figure 2.6 FADD and FADD phosphorylation are required for *Kras*-driven cell proliferation

(**A**) Representative western blot of *Luc*, K_{Luc} and KF_{Luc} MEFs immunoblotted with antibodies for FADD, Cyclin D1 and β-Actin. (**B**) Alamar blue proliferation assay of untreated *Luc*, K_{Luc} and KF_{Luc} MEFs. Graphs are comprised of 3 separate experiments. (**C**) Alamar blue proliferation assay of *Luc*, K_{Luc} and KF_{Luc} MEFs treated with 250uM CKI-7, 10uM Lonafarnib, 200nM PD0325901 or DMSO. Graphs are comprised of 3 separate experiments. (**D**) Average number of foci formed in a colony formation assay by K_{Luc} and KF_{Luc} MEFs treated with DMSO, 250uM CKI-7, 10uM Lonafarnib or 200nM PD0325901 for 2 weeks. (**E**) Fluorescence assisted cell sorting (FACS) analysis of cell cycle distribution 24 hours after treatment with DMSO, 200nM PD0325901, CKI-7 250uM or 10uM Lonafarnib in K_{Luc} and KF_{Luc} MEFs. (**F**) Representative western blot using indicated antibodies in K_{Luc} MEFs that were treated with DMSO, 250uM CKI-7, 10uM Lonafarnib or 200nM PD0325901 for 6 hours before being harvested. All data are represented as the mean $\pm$ SEM.

A.

AS | G2/M

FADD
pFADD (S194)
Cyclin B1
Cyclin D1
AURKA
PLK1
pCDC20 (S51)
pHistone H3

B.

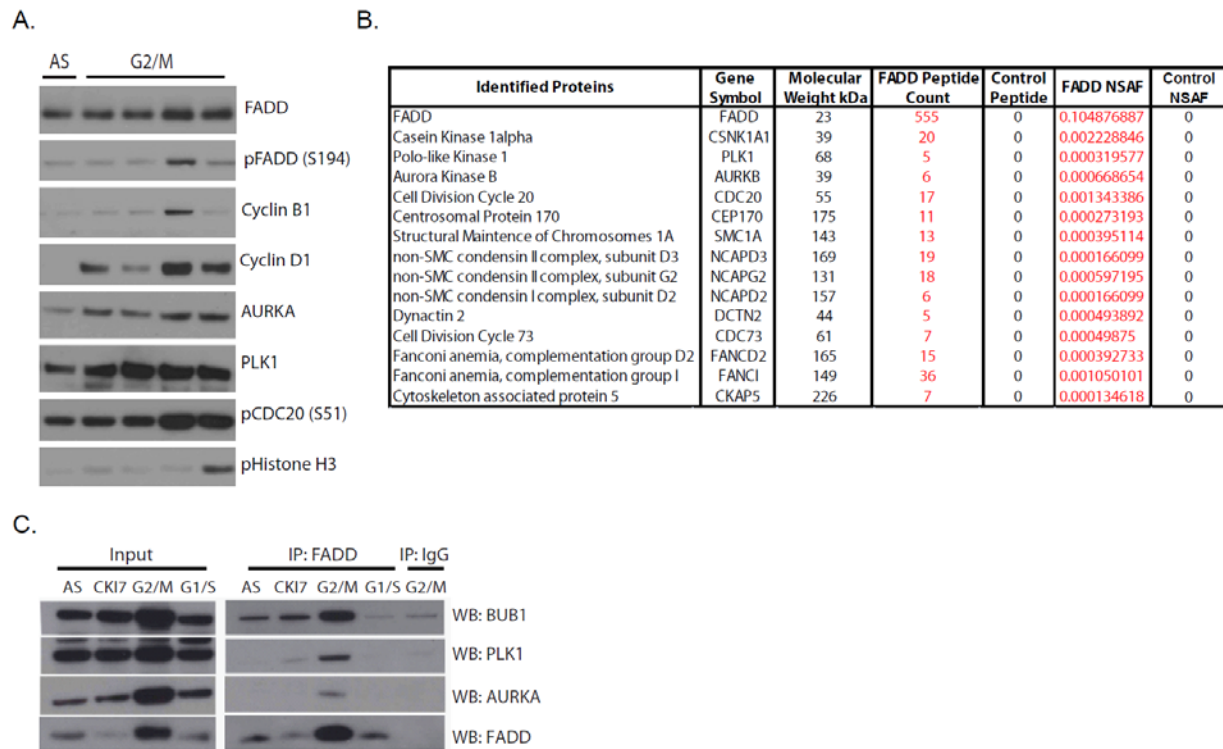| Identified Proteins	Gene Symbol	Molecular Weight kDa	FADD Peptide Count	Control Peptide	FADD NSAF	Control NSAF
FADD	FADD	23	555	0	0.104876887	0
Casein Kinase 1alpha	CSNK1A1	39	20	0	0.002228846	0
Polo-like Kinase 1	PLK1	68	5	0	0.000319577	0
Aurora Kinase B	AURKB	39	6	0	0.000668654	0
Cell Division Cycle 20	CDC20	55	17	0	0.001343386	0
Centrosomal Protein 170	CEP170	175	11	0	0.000273193	0
Structural Maintence of Chromosomes 1A	SMC1A	143	13	0	0.000395114	0
non-SMC condensin II complex, subunit D3	NCAPD3	169	19	0	0.000166099	0
non-SMC condensin II complex, subunit G2	NCAPG2	131	18	0	0.000597195	0
non-SMC condensin I complex, subunit D2	NCAPD2	157	6	0	0.000166099	0
Dynactin 2	DCTN2	44	5	0	0.000493892	0
Cell Division Cycle 73	CDC73	61	7	0	0.00049875	0
Fanconi anemia, complementation group D2	FANCD2	165	15	0	0.000392733	0
Fanconi anemia, complementation group I	FANCI	149	36	0	0.001050101	0
Cytoskeleton associated protein 5	CKAP5	226	7	0	0.000134618	0

C.

Input | IP: FADD | IP: IgG

AS CKI7 G2/M G1/S | AS CKI7 G2/M G1/S G2/M

WB: BUB1
WB: PLK1
WB: AURKA
WB: FADD

Figure 2.7 FADD interacts with key mediators of G2/M transition.
(**A**) Representative western blot using antibodies to indicated human proteins in H1975 cells after double thymidine block and subsequent release. Cells were harvested at 6, 7, 8, and 9 hours post thymidine block. The first lane was harvested asynchronous cells. (**B**) Table illustrating top cell cycle related proteins which Halo tagged FADD pulled down. NSAF is the normalized spectral abundance factor. (**C**) Representative western blot of FADD co-immunoprecipitation assay from A549 cells using antibodies against FADD, BUB1, PLK1, and AURKA. Indicated conditions include asynchronous cells, CKI-7 treated cells, nocodozole (G2/M) and hydroxyurea (G1/S) treated cells.
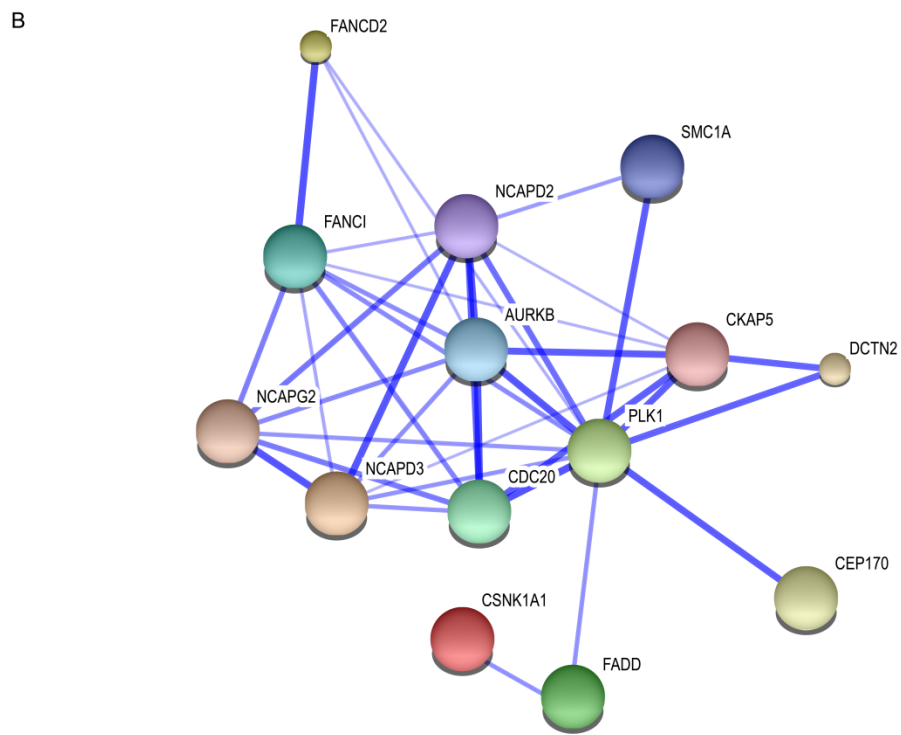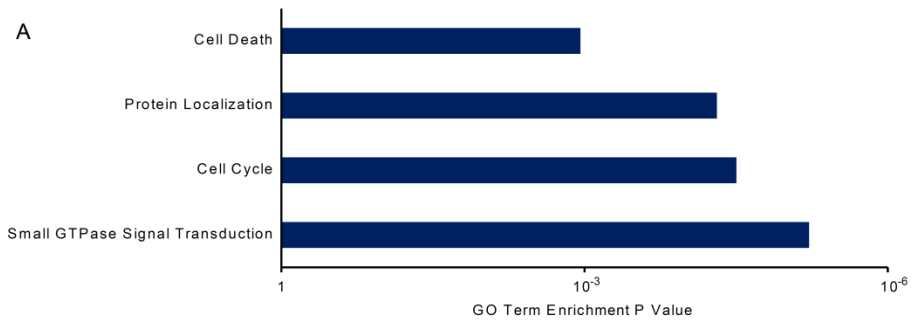
Figure 2.8 FADD interacts with proteins involved in cell cycle (**A**) Analysis of mass spectrometry data using DAVID. Top cell processes by p values as analyzed from DAVID. (**B**) Interactome of cell cycle proteins from mass spectrometry experiment prepared using STRING. Lines represent confidence of interaction.

A.

Kras — STOP — Kras^G12D (LoxP ... LoxP) → A d-Cre intranasal → Kras — Kras^G12D (LoxP)

Csnk1a1 — EXON1 — EXON2 — EXON3 — EXON4 (LoxP ... LoxP) → Csnk1a1 (LoxP) ✕

Rosa26 — STOP — Luciferase (LoxP ... LoxP) → Rosa26 — Luciferase (LoxP)

CT Imaging Time Points

Ad-Cre intranasal | CT

0 ... 5 ... 10 ... 15 ... 20

BLI | BLI | BLI

BLI Imaging Time Points

B.

C.

Week 18

D.

E.

| | HE | HE | Ki67 | FADD | CK1α | FADD | CK1α |

Luc / K_Luc / C_Luc / KC_Luc

10x | 40x | 100x

F.

Ctrl | AdCre 2x10^7 pfu | AdCre 4x10^7 pfu

CK1α
pFADD → FADD
Actin

G.

Ctrl | AdLuc 1x10^8 pfu | AdCre 1x10^8 pfu | Ctrl | AdLuc 1x10^8 pfu | AdCre 1x10^8 pfu

CK1α
P-B-Catenin (S45)
B-Catenin
P53
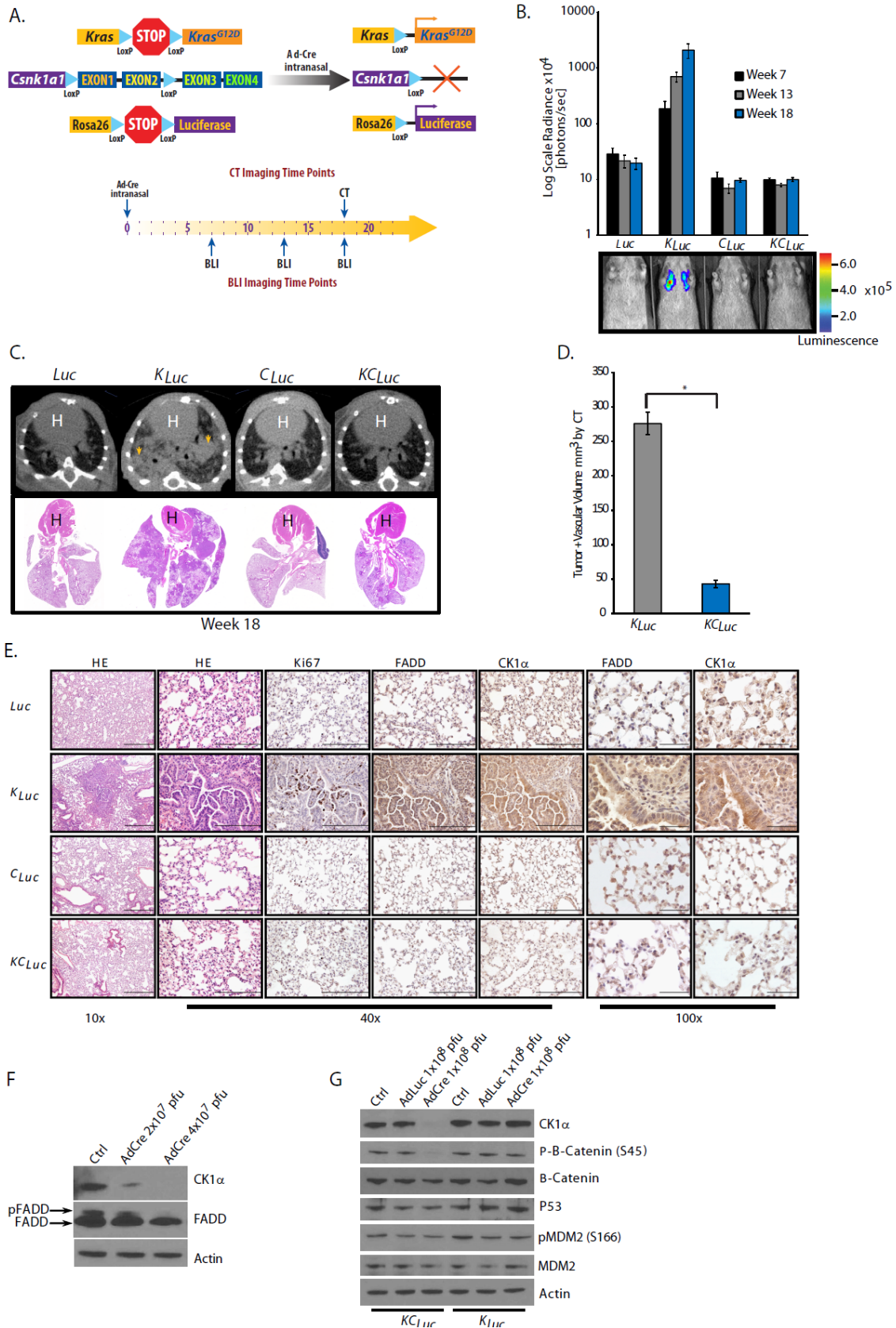pMDM2 (S166)
MDM2
Actin

KC_Luc | K_Luc

63

Figure 2.9 A requirement for CK1α in *Kras*-driven lung cancer
(**A**) Genetic strategy used to activate $Kras^{LSL-G12D}$, $Rosa26^{LSL-Luciferase}$ and delete *Csnk1a* expression in a lung specific manner. Animals were imaged for BLI and/or CT at indicated weeks post administration of Cre recombinase. (**B**) Average BLI for *Luc* (n=8), C_{Luc} (n=5), K_{Luc} (n=38), and KC_{Luc} (n=25) mice at specified times. Scale is radiance (p/sec/cm2/sr). (**C**) Representative images of CT scans of lungs from *Luc*, K_{Luc}, C_{Luc}, and KC_{Luc} animals at shown times, with H&E slide corresponding to that animal from week 18. Arrows indicate lesions. H indicates heart. (**D**) Average tumor and vascular volumes of K_{Luc} (n=8) and KC_{Luc} (n=7) analyzed from CT at indicated times. Statistical significance $*p=7.47 \times 10^{-6}$ was calculated using an unpaired Student's t-test. (**E**) Representative images of lung histology from 18 weeks post AdCre animals stained with hematoxylin and eosin (H&E) and antibodies for Ki-67, FADD and CK1α. Scale bar = 500uM for 10x, 200uM for 40x, and 50uM for 100x. (**F**) Representative western blot using antibodies against CK1α, FADD and β-actin, in KC_{Luc} MEFs that were treated with different concentrations of AdCre. pfu=Plaque forming units (**G**) Representative western blot using antibodies for indicated proteins in K_{Luc} and KC_{Luc} MEFs treated with AdCre or AdLuc (Adenovirus Luciferase)
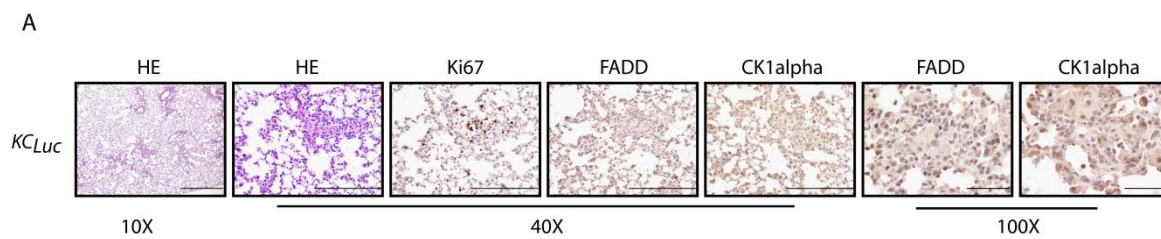
Figure 2.10 Immunohistochemistry of *Csnk1a1* null lesions reveal residual CK1α protein. Representative images of lung histology from week 18 post AdCre administration, stained with (H&E) and antibodies against Ki-67, FADD, and CK1α. Scale bar = 500uM for 10x 200uM for 40x, and 50uM for 100x.
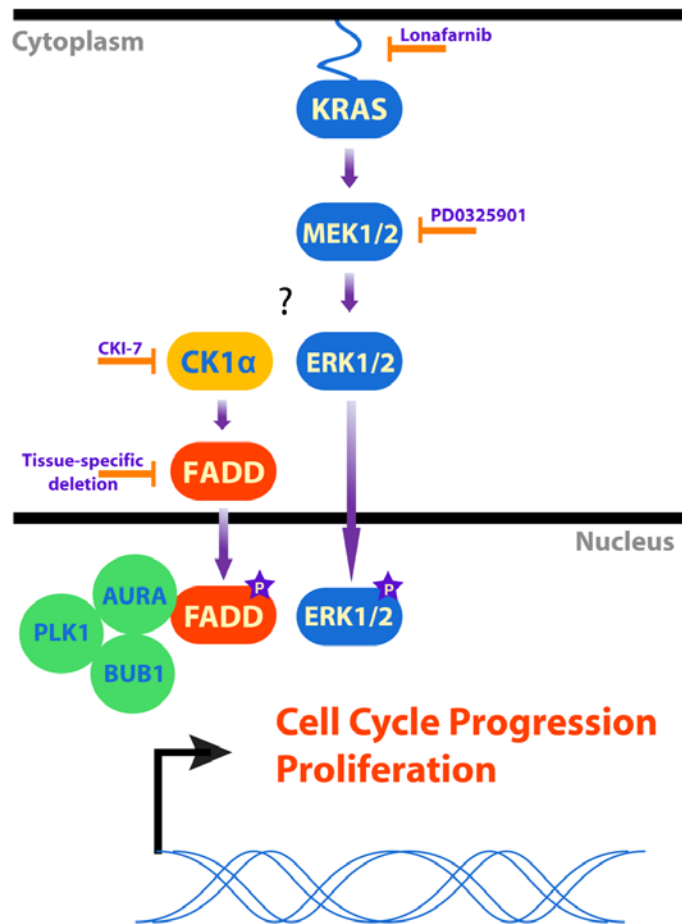
Figure 2.11 Model. Based on our data, we believe that FADD and CK1α play a necessary role in mediating KRAS mitogenic signaling in cancer. Inhibition of KRAS and MEK led to decreased FADD phosphorylation and decreased cell proliferation. Inhibition of CK1α or deletion of *Csnk1a1* also resulted in decreased growth phenotypes and decreased FADD phosphorylation. Deletion of FADD resulted in sever decrease of cell proliferation as cells were arrested in G2/M, likely since it cannot interact with key G2/M transition proteins like AURKA, PLK1 or BUB1.

2.7 References

1. Herbst, R.S., Heymach, J.V., Lippman, S.M. Lung Cancer. *N Engl Med.* **359**, 1367-1380 (2008).

2. Liu, X., Yan, S., Zhou, T., Terada, Y., Erikson, R.L. The MAP kinase pathway is required for entry into mitosis and cell survival. *Oncogene.* **23**, 763-776 (2004).

3. Chen, G., Bhojani, M.S., Heaford, A.C., Chang, D.C., Laxman, B., Thomas, D.G., Griffin, L.B., Yu, J., Coppola, J.M., Giordano, T.J., Lin, L., Adams, D., Orringer, M.B., Ross, B.D., Beer, D.G., Rehemtulla, A. Phosphorylated FADD induces NF-κB, perturbs cell cycle, and is associated with poor outcome in lung adenocarcinomas. *PNAS.* **102**, 12507-12512 (2005).

4. Bhojani, M.S., Chen, G., Ross, B.D., Beer, D.G., Rehemtulla, A. Nuclear localized phosphorylated FADD induces cell proliferation and is associated with aggressive lung cancer. *Cell Cycle.* **4**, 1478-1481 (2005).

5. Gibcus, J.H., Menkema, L., Mastik, M.F., Hermsen, M.A., de Bock, G.H., van Velthuysen, M.L., Takes, R.P., Kok, K., Alvarez Marcos, C.A., van der Laan, B.F., van den Brekel, M.W., Langendijk, J.A., Kluin, P.M., van der Wal, J.E., Schuuring, E. Amplicon mapping and expression profiling identify the Fas-associated death domain gene as a new driver in the 11q13.3 amplicon in laryngeal/pharyngeal cancer. *Clin Cancer Res.* **13**, 6257-6266 (2007).

6. Prapinjumrune, C., Morita, K., Kuribayashi,Y., Hanabata, Y., Qi Shi, Q., Nakajima, Y., Inazawa, J., Omura, K. DNA amplification and expression of FADD in oral squamous cell carcinoma. *J Oral Pathol Med.* **39**, 525-532 (2010).

7. Drakos, E., Leventaki, V., Atsaves, V., Schlette, E.J., Lin, P., Vega, F., Miranda, R.N., Claret, F.X., Medeiros, L.J., Rassidakis, G.Z. Expression of serine 194-phosphorylated Fas-associated death domain protein correlates with proliferation in B-cell non-Hodgkin lymphomas. *Hum Pathol.* **42**, 1117-1124 (2011).

8. Schrijvers, M.L., Pattje, W.J., Slagter-Menkema, L., Mastik, M.F., Gibcus, J.H., Langendijk, J.A., van der Wal, J.E., van der Laan, B.F., Schuuring, E. FADD Expression as a Prognosticator in Early-Stage Glottic Squamous Cell Carcinoma of the Larynx Treated Primarily With Radiotherapy. *Int J Radiation Oncol Biol Phys.* **83**, 1220-1226 (2012).

9. Rasamny, J.J., Allak, A., Krook, K.A., Jo, V.Y., Policarpio-Nicolas, M.L., Sumner, H.M., Moskaluk, C.A., Frierson, H.F. Jr, Jameson, M.J. Cyclin D1 and FADD as biomarkers in head and neck squamous cell carcinoma. *Otolaryngology Head Neck Surg.* **146**, 923-931 (2012).

10. Zhang, Y., Kabra, N.H., Cado, D., Kang, C., Winoto, A. FADD-deficient T cells exhibit a disaccord in regulation of the cell cycle machinery. *J Bio Chem.* **32**, 29815-29818 (2001).

11. Hueber, A.O., Zornig, M., Bernard, A.M., Chautan, M., Evan, G. A dominant negative Fas-associated death domain protein mutant inhibits proliferation and leads to impaired calcium mobilization in both T-cells and fibroblasts. *J Bio Chem.* **275**, 10453-10462 (2000).

12. Newton, K., Kurts, C., Harris, A.W., Strasser, A. Effects of a dominant interfering mutant of FADD on signal transduction in activated T cells. *Current Biology.* **11**, 273-276 (2001).

13. Alappat, E.C., Feig, C., Boyerinas, B., Volkland, J., Samuels, M., Murmann, A.E., Thronburn, A., Kidd, V.J., Slaughter, C.A., Osborn, S.L., Winoto, A., Tang, W.J., Peter, M.E. Phosphorylation of FADD at serine 194 by CKIα regulates its nonapoptotic activities. *Molecular Cell.* **19**, 321-332 (2005).

14. Zhang, Y., Rosenberg, S., Wang, H., Imtiyaz, H.Z., Hou, Y.J., Zhang, J. Conditional Fas-associated death domain protein (FADD): GFP knockout mice reveal FADD is dispensable in thymic development but essential in peripheral T cell homeostasis. *J Immunol.* **175**, 3033-3044 (2005).

15. Jackson, E.L., Willis, N., Mercer, K., Bronson, R.T., Crowley, D., Montoya, R., Jacks, T., Tuveson, D.A. Analysis of lung tumor initiation and progression using conditional expression of oncogenic K-ras. *Genes Dev.* **15**, 3243-3248 (2001).

16. Safran, M., Kim, W.Y., Kung, A.L., Horner, J.W., DePinho, R.A., Kaelin, W.G. Mouse Reporter Strain for Noninvasive Bioluminescent Imaging of Cells that Have Undergone Cre-Mediated Recombination. *Mol. Imaging.* **2**, 297-302 (2003).

17. Haines, B.B., Bettano, K.A., Chenard, M., Sevilla, R.S., Ware, C., Angagaw, M.H., Winkelmann, C.T., Tong, C., Reilly, R.F., Sur, C., Zhang, W. Micro–Computed Tomography Method to Analyze Lung Tumors in Genetically Engineered Mouse Models. *Neoplasia.* **11**, 39-47 (2009).

18. Zhang, Y., Winoto, A. A mouse Fas-associated protein with homology to the Mort1/FADD protein is essential for Fas-induced apoptosis. *Mol Cell Biol.* **16**, 2756-2763 (1996).

19. Rochat-Steiner, V., Becker, K., Micheau, O., Schneider, P., Burns, K., Tschopp, J. FIST/HIPK3: a Fas/FADD-serine/threonine kinase that induces FADD phosphorylation and inhibits fas-mediated Jun NH(2)-terminal kinase activation. *J. Exp. Med.* **192**, 1165-1174 (2000).

20. Osborn, S.L., Sohn, S.J., Winoto, A. Constitutive phosphorylation mutation in Fas-associated death domain (FADD) results in early cell cycle defects. *J Bio Chem*. **28**, 22786-22792 (2007).

21. Kim, H., Lee, H., Oh, Y., Choi, S., Hong, S., Kim, H., Lee, S., Choi, J., Hwang, J., Kim, K., Kim, H., Zhang, J., Youn, H., Noh, D., Jung, Y. The DUSP26 phosphatase activator adenylate kinase 2 regulates FADD phosphorylation and cell growth. *Nat Commun*. 5:3351 (2014).

22. Ding, L., Getz, G., Wheeler, D.A., Mardis, E.R., McLellan, M.D., Cibulskis, K., Sougnez, C., Greulich, H., Muzny, D.M., Morgan, M.B., Fulton, L., Fulton, R.S., Zhang, Q., Wendl, M.C., Lawrence, M.S., Larson, D.E., Chen, K., Dooling, D.J., Sabo, A., Hawes, A.C., Shen, H., Jhangiani, S.N., Lewis, L.R., Hall, O., Zhu, Y., Mathew, T., Ren, Y., Yao, J., Scherer, S.E., Clerc, K., Metcalf, G.A., Ng, B., Milosavljevic, A., Gonzalez-Garay, M.L., Osborne, J.R., Meyer, R., Shi, X., Tang, Y., Koboldt, D.C., Lin, L., Abbott, R., Miner, T.L., Pohl, C., Fewell, G., Haipek, C., Schmidt, H., Dunford-Shore, B.H., Kraja, A., Crosby, S.D., Sawyer, C.S., Vickery, T., Sander, S., Robinson, J., Winckler, W., Baldwin, J., Chirieac, L.R., Dutt, A., Fennell, T., Hanna, M., Johnson, B.E., Onofrio, R.C., Thomas, R.K., Tonon, G., Weir, B.A., Zhao, X., Ziaugra, L., Zody, M.C., Giordano, T., Orringer, M.B., Roth, J.A., Spitz, M.R., Wistuba, I.I., Ozenberger, B., Good, P.J., Chang, A.C., Beer, D.G., Watson, M.A., Ladanyi, M., Broderick, S., Yoshizawa, A., Travis, W.D., Pao, W., Province, M.A., Weinstock, G.M., Varmus, H.E., Gabriel, S.B., Lander, E.S., Gibbs, R.A., Meyerson, M., Wilson, R.K.. Somatic mutations affect key pathways in lung adenocarcinoma. *Nature.* **7216**, 1069-1075 (2008).

23. Okayama, H., Kohno, T., Ishii, Y., Shimada, Y., Shiraishi, K., Iwakawa, R., Furuta, K., Tsuta, K., Shibata, T., Yamamoto, S., Watanabe, S., Sakamoto, H., Kumamoto, K., Takenoshita, S., Gotoh, N., Mizuno, H., Sarai, A., Kawano, S., Yamaguchi, R., Miyano, S., Yokota, J. Identification of genes upregulated in ALK-positive and EGFR/KRAS/ALK-negative lung adenocarcinomas. *Cancer Res*. **1**, 100-111 (2012).

24. Cheng, W., Wang, L., Zhang, R., Du, P., Yang, B., Zhuang, H., Tang, B., Yao, C., Yu, M., Wang, Y., Zhang, J., Yin, W., Li, J., Zheng, W., Lu, M., Hua, Z. Regulation of PKC inactivation by FADD. *J Bio Chem*. **287**, 26126-26135 (2012).

25. Schinske, K.A., Nayti, S., Khan, A.P., Williams, T.M., Johnson, T.D., Ross, B.D., Tomas, R.P., Rehemtulla, A. A novel kinase inhibitor of FADD phosphorylation chemosensitizes through the inhibition of NF-κB. *Mol Cancer Ther*. **10**, 1807-1817 (2011).

26. Khan, A.P., Schinske, K.A., Nyati, S., Bhojani, M.S., Ross., B.D., Rehemtulla, A. High-throughput molecular imaging for the identification of FADD kinase inhibitors. *J Biomol Screen.* **15**, 1063-1070 (2010).

27.   Sun, S., Zhou, Z., Wang, R., Fu, H., Khuri, F.R. The Farnesyltransferase inhibitor Lonafarnib induces growth arrest or apoptosis of human lung cancer cells without down regulation of Akt. *Cancer Bio & Therapy.* **3**, 1092-1098 (2013).

28.   Akinleye. A., Furqan, M., Mukhi, N., Ravella, P., Liu, D. MEK and the inhibitors: from bench to beside. *J Hematol Oncol .* 6:27 (2013).

29.   Jang, M., Lee, S., Kang, N.S., Kim, E. Cooperative phosphorylation of FADD by Aur-A and Plk1 in response to taxol triggers both apoptotic and necrotic cell death. *Cancer Res.* **71**, 7207-7215 (2011).

30.   Anger, M., Kues, W.A., Klima, J., Mielenz, M., Kubelka, M., Motlik, J., Esner, M., Dvorak, P., Carnwath, J.W., Niemann, H. Cell cycle dependent expression of Plk1 in synchronized porcine fetal fibroblasts. *Mol Rep Dev.* **65**, 245-253 (2003).

31.   Huang, D.W., Sherman, B.T., Lempicki, R.A. Systematic and integrative analysis of large gene lists using DAVID Bioinformatics Resources. *Nature Protoc.* **4**, 44-57 (2009).

32.   Huang, D.W., Sherman, B.T., Lempicki, R.A. Bioinformatics enrichment tools: paths toward the comprehensive functional analysis of large gene lists. *Nucleic Acids Res.* **37**, 1-13 (2009).

33.   Qi, W., Tang, Z., Yu, H. Phosphorylation – and polo-box-dependent binding of Plk1 to Bub1 is required for the kinetochore localization of Plk1. *Mol Biol Cell.* **17**, 3705-3716 (2007).

34.   Tang, Z., Shu, H., Oncel, D., Chen, S., Yu, H. Phosphorylation of Cdc20 by Bub1 provides a catalytic mechanism for APC/C inhibition by the spindle checkpoint. *Mol Cell.* **16**, 387-397 (2004).

35.   Ricke, R.M., Jeganathan, K.B., van Deursen, J.M. Bub1 overexpression induces aneuploidy and tumor formation through Aurora B kinase hyperactivation. *J Cell Biol.* **193**, 1049-1064 (2011).

36.   Elyada, E., Pribluda, A., Goldstein, R.E., Morgenstern, Y., Brachya, G., Cojocaru, G., Snir-Alkalay, I., Burstain, I., Haffner-Krausz, R., Jung, S., Wiener, Z., Alitalo, K., Oren, M., Pikarsky, E., Ben-Neriah, Y. CKIα ablation highlights a critical role for p53 in invasiveness control. *Nature Letters.* 470, 409-413 (2011).

37.   Huart, A.A., MacLaine, N. J., Meek, D.W., Hupp, T.R. CK1alpha plays a central role in mediating MDM2 control of p53 and E2F-1 protein stability. J Biol Chem **284**, 32384-32394 (2009).

38.   Chen, L., Li, C., Pan, Y., Chen, J. Regulation of p53-MDMX interaction by Casein Kinase 1 Alpha. *Mol Cell Bio.* **15**, 6509-6520 (2005)

39. Del Valle-Pérez, B., Arqués, O., Vinyoles, M., de Herreros, A. G., Duñach, M. Coordinated action of CK1 isoforms in canonical Wnt signaling. Mol. Cell Biol. **31**, 2877–2888 (2011).

40. Adjei, A.A. Blocking oncogenic Ras signaling for cancer therapy. *J Nat Cancer Institute*. **93**, 1062-1074 (2001).

41. Riely, G.J., Kris, M.G., Rosenbaum, D., Marks, J., L,i A., Chitale, D.A., Nafa, K., Riedel, E.R., Hsu, M., Pao, W., Miller, V.A., Ladanyi, M. Frequency and distinctive spectrum of KRAS mutations in never smokers with lung adenocarcinoma. *Clin Cancer Res*. **18**, 5731-5734 (2008).

42. Ostrem, J.M., Peters, U., Sos, M.L., Wells, J.A., Shokat, K.M. K-Ras (G12C) inhibitors allosterically control GTP affinity and effector interactions. *Nature*. **7477**, 548-551 (2013).

43. Goldman, J.W., Garon, E.B. Targeting MEK for the treatment of non-small-cell lung cancer. *J Thorac Oncol*. **7**, S377-378 (2012).

44. Meng, X.W., Chandra, J., Loegering, D., Van Becelaere, K., Kottke, T.J., Gore, S.D., Karp, J.E., Sebolt-Leopold, J., Kaufmann, S.H. Central role of Fas-associated death domain protein in apoptosis induction by mitogen-activated protein kinase kinase inhibitor CI-1040 (PD184352) in acute lymphocytic leukemia cells in vitro. *J Bio Chem*. **278**, 47326-47339 (2003).

45. Fung, T. K., Poon, R. Y. C. A roller coaster ride with the mitotic cyclins. *Sem Cell Dev Biol*. **16**, 335-342 (2007).

46. Hendzel, M.J., Wei, Y., Mancini, M.A., Van Hooser, A., Ranalli, T., Brinkley, B.R., Bazett-Jones, D.P., Allis, C.D. Mitosis specific phosphorylation of histone H3 initiates primarily within pericentromeric heterochromatin during G2 and spreads in an ordered fashion coincident with mitotic chromosome condensation. *Chromosoma*. **106**, 348–360 (1997).

47. Anastas, J.N. and Moon, R.T. WNT signalling pathways as therapeutic targets in cancer. *Nature Reviews Cancer* **13**, 11-26 (2013).

48. DuPage, M., Dooley, A.L., Jacks, T. Conditional mouse lung cancer models using adenoviral antiviral delivery of Cre recombinase. *Nat Protoc.* **4**, 1064–1072 (2009).

CHAPTER 3

CONCLUSIONS

3.1 Summary of Thesis

In this thesis, I have presented evidence demonstrating the importance of FADD and its phosphorylation by CK1α in mutant *Kras*-driven lung cancer. I determined that indeed both FADD and CK1α are necessary for tumorigenesis in a mutant *Kras* dependent mouse model of lung cancer, as loss of either resulted in decreased tumor burden from abrogated proliferation. In cell culture studies I showed that FADD phosphorylation is mediated by KRAS signaling, and inhibition of this pathway or inhibition of CK1α resulted in decreased FADD phosphorylation and lower cell proliferation due to cell cycle arrest. Based on this data I believe CK1α is an attractive therapeutic target for patients with mutant *KRAS* positive NSCLC.

3.2.1 Lack of KRAS Specific Therapies

As mentioned in the introduction, there are currently no KRAS specific therapies available to the 32.2% of patients with mutant *KRAS*. Until recently, KRAS was considered an impossible to target [1]. One reason for this is the general nucleotide binding site of KRAS. Many early inhibitors acting at this site have off target effects. Second, inhibitors of farnesylation, although potent in cell cultured failed in patients again due to off target effects [1]. Recently, a set of potential compounds have been found which specifically inhibit the G12C *KRAS* mutation [2, 3]. However there are still no targeted therapies against other *KRAS* mutants. Currently, there are several clinical trials testing the inhibition of downstream targets of KRAS, such as MEK and the kinases involved in cell cycle regulation. The next sections describe the state of current state of the art drugs and their respective clinical trials.

3.2.1.1 *KRASG12C* Inhibitors

Recently, two groups found success in inhibiting the *KRAS* G12C mutation; both groups discovered compounds which affect the nucleotide binding site in KRAS by exploiting the Cys 12 residue [2, 3]. Ostrem et al., 2013 found compounds that allosterically inhibit GTP binding by disturbing both switch I and II resulting in an increased affinity for GDP [2]. Separately in 2014, Hunter et al developed irreversible inhibitors which covalently bind to Cys 12 [3]. These findings are very exciting, as KRAS could be targeted specifically for the first time. It also gives hope for patients with this mutation, although it will be several years before this will become a reality. The need remains to develop inhibitors targeting the other G12 mutations in *KRAS*. Finding inhibitors which target the G12D mutation may be feasible since the negatively charged aspartic acid could be utilized, but the G12V mutation may prove to be more difficult to target. Importantly, inhibitors of downstream targets would benefit patients regardless of their *KRAS* mutation.

3.2.1.2 MEK Inhibitors

As mentioned earlier, there is ongoing research into downstream targets of the EGFR/KRAS pathway. MEK is one such downstream target. Currently, there are several trials underway to test the efficacy of MEK inhibitors as monotherapies as well as in combination therapies with docetaxel. At present, there are several compounds currently in clinical trials for targeting MEK in mutant *KRAS* positive NSCLC. The two I will focus on are Selumetinib and Trametinib which are selective oral inhibitors of MEK1/2 [4]. Selumetinib has been entered into a phase III trial in combination with docetaxel after a successful phase II. In the phase II trial, patients who were treated with selumetinib and docetaxel (n=44) saw an improvement in progression-free survival of 5.2 months versus 2.1 months of patients treated with docetaxel and placebo (n=43) [5]. The combination treatment also had a median overall survival of 9.4 months as compared to 5.2 months of docetaxel and placebo [5]. However, many patients (18%) on the combination therapy suffered from febrile neutropenia as well as a general increase in hospital visits as compared to the docetaxel only group [4, 5]. Currently there is an ongoing phase III trial for this treatment in patients with late stage and mutant *KRAS* NSCLC (NCT01933932) [4, 6]. Trametinib has been approved in

combination treatment of patients with melanoma **[4]** and several phase I clinical trials in NSCLC have been completed **[4, 7]**.

Although there has been partial success with selumetinib, several trials involving MEK inhibitors failed **[8]**.This was due to increased toxicity, such as rash, diarrhea, nausea. Depending on the inhibitor, serious neurotoxicity (PD3025901), rare left ventricular cardiac dysfunction (tramentinib), and disappointing tumor response also occurred **[8]**. MEK inhibitors remain the next best in treatment for KRAS-driven lung cancer, however new inhibitors with less toxicity are needed as well as optimal therapy regimens.

3.2.1.3 AURKA and PLK1 Inhibitors

Polo-like Kinase 1 (PLK1) and Aurora Kinase A (AURKA) are important regulators of cell cycle progression and each have several roles. PLK1 signaling affects mitotic entry, centrosome maturation, spindle assembly, APC/C regulation and cytokinesis **[9, 10]**. PLK1 overexpression in NSCLC has been shown to correlate with poor survival in patients **[11]**. Currently there are several clinical trials with potent PLK1 inhibitors. Although these inhibitors, such as BI 2536, BI 6727, are potent and selective for PLK1, PLK1 inhibitors have only shown modest clinical efficiency with very few NSCLC patients responding to treatment **[12-15]**. These inhibitors also suffer from high toxicity such as neutropenia, nausea, fatigue, leucopenia and thrombocytopenia **[12-15]**.

Similarly to PLK1 inhibitors, AURKA inhibitors also have not proved to be efficient targets in clinical trials and suffer from high toxicity **[16]**. Like PLK1 inhibitors the most common side effect is neutropenia. Furthermore, AURKA has not been demonstrated to be an oncogene **[16]**. Although, there are several reports where high levels of AURKA in cell culture potentiates mutant *KRAS* transformation, increased levels of AURKA did not lead to transformed cells **[16, 17]**. There are several second generation AURKA inhibitors in phases I and II for solid tumors and it will be interesting to see the outcomes.

Interestingly, both kinases bind to FADD (**Fig. 2.7**) and phosphorylate FADD **[18, 19]**. Inhibition of these kinases results in G2/M arrest and a decrease in FADD phosphorylation. Our depletion of CK1α in a mouse model of lung cancer led to similar

results as FADD depletion and led to a significant loss of FADD phosphorylation. It is unclear how important PLK1 or AURKA is in regulating FADD in this context. Regardless, current therapies against both kinases are proving to be highly toxic without useful clinical efficiency in NSCLC, indicating the need for new inhibitors or even different targets.

3.2.2 CK1α as a Therapeutic Target

We have demonstrated that inhibition of CK1α is a viable method to treat mutant *Kras*-driven lung cancer. Inhibition or depletion of CK1α decreased cell proliferation as a result of cell cycle arrest in cell culture prevented the formation of lesions in the KC_{Luc} mouse model. In BaF3 cells, expression of CK1α was recently observed to be necessary for *KRAS* G12V driven cell proliferation [20]. CK1α was required for the formation of plasamacytomas in a mouse model, and animals with low expression of CK1α lived longer than animals with both mutant *KRAS* and CK1α expression [20]. Together these data indicate CK1α as an attractive downstream target of mutant *KRAS*-driven cancers.

3.2.3 Need for New CK1α Inhibitors

Currently there are several CK1 inhibitors available to researchers. However, these inhibitors are not satisfactory due to problems with affinity, bioavailability and selectivity. CK1-7 is a widely used CK1 inhibitor which suffers from a low IC50 of 6 uM and poor cellular uptake [21, 22]. CKI-7's poor uptake necessitated the high concentration used in this thesis (250uM). Another commonly used inhibitor is D4476. D4476 has an IC50 of 0.3uM molar affinity for CK1α [22], however it has poor bioavailability and in cell based assays has decreased activity (20-50uM) [23, 24]. Both inhibitors also have off target effects. CKI-7 is a 6uM inhibitor of SGK, and other CK1 isoforms and D4476 has been shown to inhibit ALK5, p38, and CK1ε [22, 23, 25].

While these inhibitors are widely used, their issues highlight a need for new and better drugs. New CK1α inhibitors are inadvertently being discovered in the effort to synthesize new CK1ε/δ inhibitors for their role in circadian rhythm [24]. One potential CK1α inhibitor is a compound called Bischof-5, [26, 27]. Subsequent compounds derived from Bischof-5 confer nanomolar affinity for CK1α. At least three compounds that have nanomolar affinity for CK1α (Compound 1: 163.4nM; Compound 5: 228.6nM;

Compound 6: 340.2nM) [27] which is more sensitive than either CK1-7 or D4476 (6uM and 0.3-20uM, [23, 24]) [27]. Although these compounds are more specific for the CK1ε/δ isoforms, these agents provide a starting point for developing specific CK1α inhibitors.

3.3 Future Directions

In the work presented in this dissertation, significant progress has been made in confirming FADD and its phosphorylation by CK1α as important downstream mediators of *Kras* signaling and CK1α as a promising targeting this pathway. However, further work needs to be carried out to demonstrate the benefits of inhibiting FADD phosphorylation in other contexts, such as NSCLC with other genetic drivers or even other cancers. Both p53 loss and abrogated EGFR also prevalent in lung cancer as discussed in section 1.2.3.4. To better stratify patients for targeted therapies, studying the role of FADD in a mouse model of p53 loss or overexpressed/mutant *EGFR* would be an important future direction. I believe that loss of FADD or inhibition of CK1α in EGFR dependent lung cancer may be similar to the results we found in this thesis, since KRAS is downstream of EGFR.

Another interesting future direction would be to confirm FADD interacting proteins from our Mass Spectrometry data. As mentioned in Chapter 2, many of these proteins are involved in G2/M transition of the cell cycle. FADD may play a role in chromosome condensation and sister chromatid cohesion; mass spectrometry reveals FADD interacts with proteins from both the cohesion and condensin complexes (**Fig. 2.7B**). Both cohesion and condensin complexes are important for proper chromosome segregation [28]. Phosphorylated FADD has been shown to be localized to the mitotic spindle in mitosis [29]. If FADD is a necessary component in these complexes, it is possible that cells arrest in G2/M due to improper mitotic spindle formation/separation when FADD is lost.

In summary, FADD and CK1α pose as new therapeutic targets for patients with mutant *KRAS* lung cancer.

3.4 References

1.   Downward, J., *RAS's cloak of invincibility slips at last?* Cancer Cell, 2014. **25**(1): p. 5-6.

2.   Ostrem, J.M., et al., *K-Ras(G12C) inhibitors allosterically control GTP affinity and effector interactions.* Nature, 2013. **503**(7477): p. 548-51.

3.   Hunter, J.C., et al., *In situ selectivity profiling and crystal structure of SML-8-73-1, an active site inhibitor of oncogenic K-Ras G12C.* Proc Natl Acad Sci U S A, 2014. **111**(24): p. 8895-900.

4.   Stinchcombe, T.E. and G.L. Johnson, *MEK inhibition in non-small cell lung cancer.* Lung Cancer, 2014.

5.   Janne, P.A., et al., *Selumetinib plus docetaxel for KRAS-mutant advanced non-small-cell lung cancer: a randomised, multicentre, placebo-controlled, phase 2 study.* Lancet Oncol, 2013. **14**(1): p. 38-47.

6.   www.clinicaltrial.gov

7.   Infante, J.R., et al., *Safety, pharmacokinetic, pharmacodynamic, and efficacy data for the oral MEK inhibitor trametinib: a phase 1 dose-escalation trial.* Lancet Oncol, 2012. **13**(8): p. 773-81.

8.   Goldman, J.W. and E.B. Garon, *Targeting MEK for the treatment of non-small-cell lung cancer.* J Thorac Oncol, 2012. **7**(16 Suppl 5): p. S377-8.

9.   Medema, R.H., C.C. Lin, and J.C. Yang, *Polo-like kinase 1 inhibitors and their potential role in anticancer therapy, with a focus on NSCLC.* Clin Cancer Res, 2011. **17**(20): p. 6459-66.

10.   Barr, F.A., H.H. Sillje, and E.A. Nigg, *Polo-like kinases and the orchestration of cell division.* Nat Rev Mol Cell Biol, 2004. **5**(6): p. 429-40.

11.   Wolf, G., et al., *Prognostic significance of polo-like kinase (PLK) expression in non-small cell lung cancer.* Oncogene, 1997. **14**(5): p. 543-9.

12.   Yim, H., *Current clinical trials with polo-like kinase 1 inhibitors in solid tumors.* Anticancer Drugs, 2013. **24**(10): p. 999-1006.

13.   Rudolph, D., et al., *BI 6727, a Polo-like kinase inhibitor with improved pharmacokinetic profile and broad antitumor activity.* Clin Cancer Res, 2009. **15**(9): p. 3094-102.

14.   Schoffski, P., et al., *A phase I, dose-escalation study of the novel Polo-like kinase inhibitor volasertib (BI 6727) in patients with advanced solid tumours.* Eur J Cancer, 2012. **48**(2): p. 179-86.

15.   Sebastian, M., et al., *The efficacy and safety of BI 2536, a novel Plk-1 inhibitor, in patients with stage IIIB/IV non-small cell lung cancer who had relapsed after, or failed, chemotherapy: results from an open-label, randomized phase II clinical trial.* J Thorac Oncol, 2010. **5**(7): p. 1060-7.

16.   Kollareddy, M., et al., *Aurora kinase inhibitors: progress towards the clinic.* Invest New Drugs, 2012. **30**(6): p. 2411-32.

17.   Tatsuka, M., et al., *Overexpression of Aurora-A potentiates HRAS-mediated oncogenic transformation and is implicated in oral carcinogenesis.* Oncogene, 2005. **24**(6): p. 1122-7.

18.   Jang, M.S., et al., *Cooperative phosphorylation of FADD by Aur-A and Plk1 in response to taxol triggers both apoptotic and necrotic cell death.* Cancer Res, 2011. **71**(23): p. 7207-15.

19.   Jang, M.S., et al., *Phosphorylation by polo-like kinase 1 induces the tumor-suppressing activity of FADD.* Oncogene, 2011. **30**(4): p. 471-81.

20.   Hu, Y., et al., *CSNK1alpha1 mediates malignant plasma cell survival.* Leukemia, 2014.

21.   Chijiwa, T., M. Hagiwara, and H. Hidaka, *A newly synthesized selective casein kinase I inhibitor, N-(2-aminoethyl)-5-chloroisoquinoline-8-sulfonamide, and affinity purification of casein kinase I from bovine testis.* J Biol Chem, 1989. **264**(9): p. 4924-7.

22.   Rena, G., et al., *D4476, a cell-permeant inhibitor of CK1, suppresses the site-specific phosphorylation and nuclear exclusion of FOXO1a.* EMBO Rep, 2004. **5**(1): p. 60-5.

23.   MacLaine, N.J., et al., *A central role for CK1 in catalyzing phosphorylation of the p53 transactivation domain at serine 20 after HHV-6B viral infection.* J Biol Chem, 2008. **283**(42): p. 28563-73.

24.   Badura, L., et al., *An inhibitor of casein kinase I epsilon induces phase delays in circadian rhythms under free-running and entrained conditions.* J Pharmacol Exp Ther, 2007. **322**(2): p. 730-8.

25.   Knippschild, U., et al., *The CK1 Family: Contribution to Cellular Stress Response and Its Role in Carcinogenesis.* Front Oncol, 2014. **4**: p. 96.

26. Bischof, J., et al., *2-Benzamido-N-(1H-benzo[d]imidazol-2-yl)thiazole-4-carboxamide derivatives as potent inhibitors of CK1delta/epsilon.* Amino Acids, 2012. **43**(4): p. 1577-91.

27. Richter, J., et al., *Difluoro-dioxolo-benzoimidazol-benzamides As Potent Inhibitors of CK1delta and epsilon with Nanomolar Inhibitory Activity on Cancer Cell Proliferation.* J Med Chem, 2014. **57**(19): p. 7933-46.

28. Jeppsson, K., et al., *The maintenance of chromosome structure: positioning and functioning of SMC complexes.* Nat Rev Mol Cell Biol, 2014. **15**(9): p. 601-14.

29. Alappat, E.C., et al., *Phosphorylation of FADD at serine 194 by CKIalpha regulates its nonapoptotic activities.* Mol Cell, 2005. **19**(3): p. 321-32.

APPENDIX

Author Contributions

Chapter 2:

This chapter is in press for Science Signaling, along with the following authors: Katrina A. Sebolt, Benjamin A. Hoff, Jennifer L. Boes, Danette L. Daniels, Kevin A. Heist, Craig J. Galbán, Rajiv M. Patel, Jianke Zhang, David G. Beer, Brian D. Ross, Alnawaz Rehemtulla, and Stefanie Galbán

For this chapter Brittany Bowman, Brian Ross, Alnawaz Rehemtulla and Stefanie Galban planned and wrote the paper. Brittany Bowman   Katrina A. Sebolt, Benjamin A. Hoff, Jennifer L. Boes, Danette L. Daniels, and Kevin A. Heist planned and performed experiments.   Rajiv M. Patel performed pathological analysis of mouse lung cancer histology. Craig J. Galbán, Jianke Zhang, and David G. Beer provided material, expertise and discussions over the course of the experiments and during the preparation of the manuscript.

All figures generated in this chapter were done by Brittany Bowman and Katrina Sebolt. Figures 2.1-2.6, 2.8-2.11 by Brittany Bowman and Figure 2.7 by Katrian Sebolt.